2012

# A Fractal Analysis of the Detection of Glucose Molecules on Biosensor Surfaces

Lokesh Taneja

# A FRACTAL ANALYSIS OF THE DETECTION OF GLUCOSE MOLECULES ON BIOSENSOR SURFACES

A Thesis

Submitted to the Graduate School

In partial fulfillment of the requirement for the

Degree of Master of Science in Engineering

The University of Mississippi

LOKESH TANEJA

May 2012

ABSTRACT

A fractal analysis for the binding and dissociation of glucose molecules to different biosensor surfaces is presented. The sensors contain immobilized glucose oxidase enzymes that have an affinity for the glucose molecules in solution. Data for different modified biosensors is modeled and analyzed, and a single, dual or triple-fractal analysis is applied where adequate. The binding and dissociation kinetics coefficient where applicable are calculated for each of models along with the fractal dimensions. When both binding and dissociation phases are present, the affinity, K of the receptor to the glucose molecule is calculated and its variation with the fractal dimension ratio is observed. A trend between the binding and dissociation coefficients and their respective fractal dimensions are observed, and the values used to draw conclusions of the degree of heterogeneity on the surfaces of the biosensors in relations with the concentration of glucose present in solution.

ACKNOWLEDGMENTS

I would like to express my gratitude and appreciation to my supervisor, Dr. Ajit Sadana, whose expertise, patience and guidance, added considerably to my graduate experience. His advice and encouragement was invaluable. I doubt I will ever be able to convey how grateful I am for all his support, but I owe him my sincere gratitude from the bottom of my heart.

Very special thanks goes out to my thesis defense committee members Dr. Clint Williford and Dr. Wei-Yin Chen for taking time out and reviewing my thesis and playing a key importance in the defense.

I would also like to thank all my family, friends and classmates without whom I wouldn't be where I am today and of course Mrs. Ann Pringle of the Chemical department, who selflessly assisted me with all my problems and provided a very light environment even during the most stressful conditions.

Lastly I would like to thank Dr. Clint Williford and the entire Chemical Engineering department for providing me with financial support and a very hospitable environment to learn in, it has truly been a very memorably journey here at Ole miss pursuing my graduate degree.

TABLE OF CONTENTS

CHAPTER PAGE

LIST OF TABLES

TABLE PAGE

LIST OF FIGURES

FIGURE PAGE

# CHAPTER 1

# INTRODUCTION

## 1.1 What are Biosensors?

In order to maintain the metabolism in living things, molecules must keep transporting electrons. This movement of electrons within the molecules can be observed by using electrochemistry. Biosensors are analytical devices that contain biological responsive material embedded in transducers that convert biological response into an electrical signal. These biological materials also known as biomolecules are used as a whole and include but are not limited to enzymes, receptor proteins, tissue, nucleic acid and microorganisms themselves. Each of the different biomolecules is used to identify a change in the target molecule. This change could be concentration of a substance or any other biological change of interest that doesn't use a biological system directly.

There is an ever-increasing demand for biosensors in various fields as their different applications in these fields are slowly being discovered. Some of these areas include medicine, biotechnology and environmental control (e.g. for detection of greenhouse gases and pollutants in water). The main characteristic of the biosensors responsible for this high demand and usability are the receptors that offer shape-specific recognition, hence making the sensor highly sensitivity and specific in nature. One of the main advantages that biosensor has over other analytical methods such as liquid and gas chromatography is that they can be used in situations where the molecule to be measured is in micro concentrations i.e. $10^{-9}$ to $10^{-18}$ M (Byfield et al. 1994). However, like all other analytical methods, biosensor uses have a disadvantage in application, and that is that a

small adjustment in the experimental matrix could possibly result in a drop in the affinity of the interaction between the analyte and receptor. This would in turn result in inaccurate readings. On the other hand one of the main advantages of biosensors that is applicable to this thesis, is that the reactions can be monitored in real time. This means that binding and dissociation of complexes on the sensor chip surface can be studied, enabling the modeling of kinetics and determining the mechanism of the complex reactions.

Glucose sensing is an important area due to its role in medicinal and industrial fields. It is important to detect blood sugar levels rapidly in order to control and treat diabetes mellitus (DM) in humans. This raises the need for simple, cost-effective, accurate, portable, rapid and easily regenerated glucose sensors that are socially important as a result of the rapidly increasing populations of people affected by diabetes which represents approximately 6.4 % of the world's population (Yoo et al. 2010).

Biosensors are growing at an annual rate of 60 % and the health-care industries, food quality appraisals and environmental monitoring mainly contribute to this growth. The approximate world analytical market is twelve billion dollars per year of which nearly a third is in the medical area. Of this total market, only approximately 0.1 % accounts for the use of biosensors, hence exhibiting the vast potential growth in this area. Research and development in this field is broad and involves areas such as physical chemistry, electrochemistry, bioreactor science and biochemistry. Majority of the focus is on amperometric biosensors and colorimetric paper enzyme strips. Although, at present more focus is being given to the research of the different transducer types and their application to biosensors (Chaplin et al. 1990).

1.2 Glucose Biosensor

Typical glucose biosensors consist of enzymes as the biological responsive material and are used to evaluate glucose levels in human blood. The enzyme glucose oxidase recognizes the glucose molecule and catalyzes the oxidation to gluconolactone, which hydrolyses to gluconic acid in water. This enzyme substrate interaction occurs with the glucose molecule being bonded to the cleft shaped active sites of the glucose oxidase enzyme via multiple weak attractions. Oxygen is consumed during the reaction producing hydrogen peroxide simultaneously:

$$C_6H_{12}0_6 + O_2 \xrightarrow{\text{Glucose Oxidase}} C_6H_{10}O_6 + H_2O_2$$

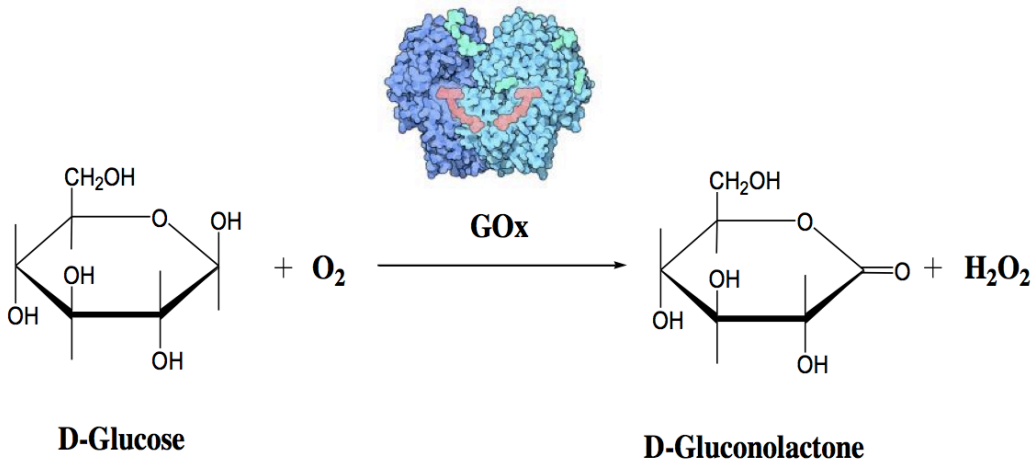


The glucose concentration can be determined by either the change in hydrogen peroxide released or the concentration of the dissolved oxygen. As can be observed from the above formula, the decrease in oxygen concentration and the increase in that of the hydrogen peroxide are proportional to the glucose concentration.

Figure 1 below shows the main structure of a typical glucose biosensor. The sensor contains an anode and electrode that are dipped in an electrolyte. The outer layer of the cathode end is generally constructed with a semi-permeable membrane that is permeable to incoming gas (oxygen molecules) but impermeable to outgoing electrolyte solution, this

prevents leakage of the electrolyte. The semi-permeable gas membrane is shielded by an oxygen deprived membrane that immobilizes the water-soluble enzyme thus preventing it from an outflow upon repeated use. A suitable material is used for the anode to enable regeneration of oxygen at different electrochemical potentials.

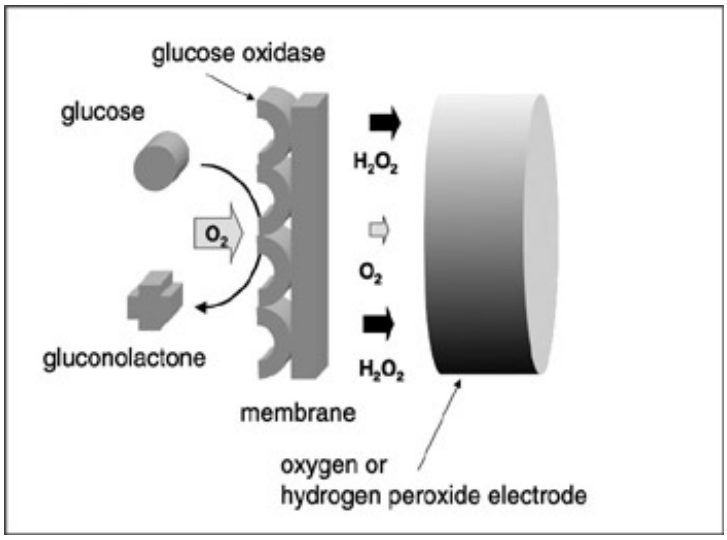


Figure 1: Schematic of a glucose biosensor (Sienko et al. 2003)

In the above figure, oxygen is consumed as glucose gets oxidized to gluconolactone at the membrane and hydrogen per oxide is produced simultaneously. The electrode can record the concentrations of both these gases. After every run the membrane is cleaned of the substrate and the sensor prepared for reuse, this reduces the lifetime of the sensor and the only way to minimize this is to prevent the enzyme from leaking out of the membrane.

The enzyme immobilized on the membrane uses up the oxygen for oxidation when glucose is present. This drop in oxygen concentration near the membrane alters the electric signal current that is transmitted by the oxygen electrodes. A transducer in the form of an electrical signal then records this change in concentration of oxygen. The transducer bound together with the recognition molecule (enzyme) makes up the biosensor.

The components of the glucose biosensor i.e. cathode and anode material, electrolyte, membranes and buffer solutions etc. are altered as required in different experiments. These will be discussed in details in the further chapters.

## 1.3 Use of Fractals in Biosensors

The best way to describe a fractal is, “an object or quantity that displays self-similarity, in a somewhat technical sense, on all scales” (Wolfram mathworld). All the scales do not necessarily have to have the exact same identical structure but must have the same kind of structure. Plotting this quantity on a log vs scale graph produces a straight line whose slope is the fractal dimension. The fractal dimension characterizes the fractal. The nature of the fractal dimension is dependent on the power-law and is restricted to three-dimensional space owing to the 3-D coordinate system. The space-filling ability of the system dictates the fractal dimension number of the system i.e. a 3-D fractal system may have the fractal dimension of three or less.

The use of biosensors is not only limited to the detection of the analyte-receptor complex but can also be used to model kinetics on these interactions. The modeling of these kinetics are discussed further in the Theory section of this thesis.

# CHAPTER 2

# LITERATURE REVIEW

## 2.1 Background of Biosensors

The first biosensor ever to be created was that for the detection of glucose, after this the structural component of the biosensor was known and exploited for the detection of various other target molecules. The most crucial development in the biosensor area has been that of restricting the receptive molecule in a membrane, this enabled the use of various materials such as antibodies, microorganisms etc. as recognition elements, allowing to develop a broader range of analyte-receptors for detection. Karube et al. (1971) was the first to electrically immobilize the enzyme into a membrane made of collagen.

The transducers used to relay the biological process into electric output were electrodes, thermistors, surface acoustic wave (SAW) or even a quartz crystal microbalance. The choice was dependent on the type of molecule to be detected. The electrodes could donate or take up electrons as required for oxidation, and this change in electrons was recorded by a potentiostat connected to the electrode that generated a change in current (Norouzi et al. 2010).

The membranes used in the biosensor are of two types; one that has an embedded catalyst and the other that embeds a compound (enzymes, microorganisms) that has a high affinity for biomolecules. In both cases electrochemical devices measure the change in concentration of hydrogen peroxide and dissolved oxygen. In rare cases is the output measured based on changes in optical phenomena or heat generated. The heat is generated

from the energy release when glucose gets oxidized, and this rise in temperature is recorded by a thermistor that acts as a transducer in this case. A biosensor that records changes based on heat is more tedious to service and regenerate as the membrane used in such a sensor should have a measured permeability, thickness and enzyme quantity to have an effective relay of physical change into an electrical output.

The most commercialized and widely used glucose sensor today, is the one that uses electrodes to detect changes in concentration of dissolved oxygen or hydrogen peroxide. The shortened lifespan of the enzyme and effect of matrix on the signal are some of the key problems that have influenced the limited use of biosensors in today's world. These problems can be resolved by microfabricating the biosensor, which involves separate fabrication processes for both the membrane and the transducer. Fabricating the membrane involves immobilizing the enzyme and Sienko et al. (2003) state that this can be attained in 3 ways: crosslinking, binding to resin and encapsulation. Crosslinking involves a compound with two or more aldehyde functions (e.g. glutaraldehyde) forming covalent bonds with the amino acid groups of the enzyme forming an insoluble membrane. Binding to resin involves the formation of the same covalent bonds as the cross linkage, only difference is that instead of aldehyde functions, the resin surface contains either amino-, carboxyl- or thiol groups. The third way, encapsulation involves the encapsulation of the enzyme in a matrix of insoluble polymer, that surrounds the enzyme and only allows the substrate to diffuse through for reaction. This in turn causes the rate of reaction to be dependent on the rate of diffusion of the substrate. It is therefore desirable to have a slimmer membrane.

Since all these processes are manual, it is difficult to use these ways; hence Shinohara et al. (1988) developed an electrical method to solve this problem. They did this by dipping a gold and platinum electrode into a solution of the enzyme and aniline followed by electro-

oxidation, which formed a membrane made of polyalinine on the surface which contained the enzyme and was only permeable to ions the size of oxygen.

In the late 90s, the increase in the aging population and frequency of number of people getting diabetes in Japan triggered the need for a frequent monitoring, disposable and less painful glucose sensor. Karube and group (1992) developed a microfabricated glucose biosensor that was small in size and utilized plasma polymerized membrane (PPM) that is a pinhole free homogeneous membrane. This immobilization method allows for the attaching of the functional chemical groups over a small area under vacuum, and has shown great and immediate responses to glucose levels in the blood. The small area also enabled the easy reproducibility of the membrane.

## 2.2 History of Fractals

Since 1800s mathematicians and scientist have been challenged with the concept of learning and understanding non-linear systems. They had mastered the linear system concept and the need to go more into depth with the non-linear systems was the fact that the world that we live in is actually a non-linear system. One of the methods they discovered to describe these non-linear systems is by using the fractal theory. The word fractal is actually english for a Latin word derivate “fractus” that means irregular and fragmented.

In 1962, a French American mathematician set out to solve a mathematical problem related to fluctuation of prices and the volatile stock market. This mathematician during his lifetime not only gained an IBM Fellow award, but also contributed immensely towards the development of IBM’s supercomputer “Watson”. Benoit Mandelbrot was a Masters graduate from California Institute of Technology and developed theories that lead to the discovery of fractals. He developed a theory that suggested that long term fluctuations represent the actual fluctuations in economy and that short term fluctuations were random and as a result of

speculations. He observed that these random fluctuations were out of the norm, and devised a theory that both short and long-term fluctuations actually shared the same statistics. Based on this, he derived a mathematical model for predicting trends in stock markets. He then further went ahead and successfully applied his model to other fields (Mandelbrot 1983).

Mandelbrot named the system describing set of values as Mandelbrot-set. As he followed the work of his professor, Gaston Julia, who in 1917 published theories related with bifurication and Verhulst processes but could not execute them due to lack of sophisticated computers capable of performing numerous calculations at once, Mandelbrot proposed that the solution to these problems were contained within the complex number set. This set of numbers followed the recursion law, hence their resulting values would map onto the original values. The equation is represented below:

$$Z_n = Z_{n-1}^2 + C$$

Where C is any point on the complex plane. A visual description of how the numbers fluctuate as iteration is carried out is better explained with the aid of the figure 2.

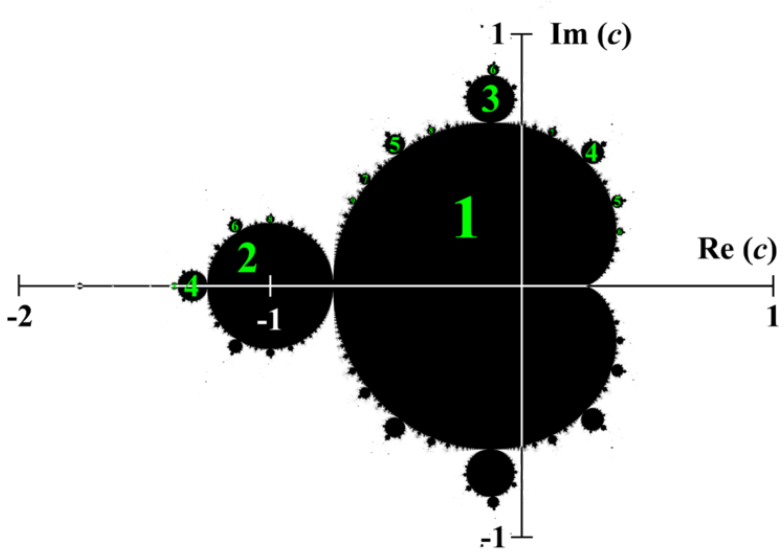


Figure 2: Mandelbrot set and periodicities of orbits (Mandelbrot, B.B. 1983)

The numbers that are contained in the black coloring represent the Mandelbrot set, and return to zero when iterated. The numbers outside the black enclosed area generally go off to infinity when iterated. He called this “The fractal geometry of nature.”

Fractals are beneficial as they describe structures and shapes with the use of formulas. For example a mathematician with the use of formulas could precisely describe a shape of a tree the exact same way a normal person would describe it. Fractals are gaining popularity for application in various science fields and one of the main areas it is of interest is in the health sciences. In the following chapters we apply fractals to one of the areas contributing to a challenging medical health problem; Diabetes mellitus.

# CHAPTER 3

## FRACTAL THEORY

In the glucose biosensor, the molecule to be detected is glucose (analyte) and the appropriate enzyme receptor is immobilized on the sensor surface. The interaction between the receptor and the analyte is detected and recorded. A heterogeneous distribution on the sensing surface is included to minimize the limitations offered by diffusion. The heterogeneity could be as a result of inherent irregularities on the sensor surface, nonspecific binding and mixture of receptor or analytes on the sensing surface.

The effects of the limitations of diffusion and the degree of heterogeneity on the surface of the biosensor both influence the binding and dissociation kinetics. These will be coupled together and their presence accounted for by the use of fractals (Havlin 1989).

Fractals are systems that are disordered and these are described by non-integral dimensions (Pfeifer et al. 1989). Fractals are generally smaller than the dimension size they are embedded in, and this means that an increase in heterogeneity on the surface of the sensor would in turn lead to an increase in the fractal dimension. The fractal dimension can never be a negative number and a low value indicates that the surface exists as a cantor-like dust (Sadana et al. 2011). Hence the heterogeneity on the biosensor surface will be characterized using fractal dimensions.

Diffusion that is controlled on the surface of the sensor during the reaction generally occurs on clusters and exhibits fractal-like kinetics (Kopelman, R., 1988). These kinetics show irregular reaction orders and rate coefficients that is dependent on time. The fractal dimension can characterize an irregular surface as long as it exhibits scale invariance.

Fractals are self-similar mathematical objects of scale that have nontrivial geometric properties (Markel et al. 1991). Following are the details of Havlin's review and analysis of the diffusion of the reactants towards fractal surfaces.

## 3.1 Single-Fractal Analysis

3.1.1 Binding rate coefficient - Havlin (1989) showed that the product (analyte-receptor) formed by the reaction, is caused due to the diffusion of the analyte from a homogenous solution to the solid surface of the sensor (coated with the receptor). This product (analyte-receptor) concentration increases with time as follows:

$$(\text{analyte.receptor}) \sim \begin{cases} t^{(3-D_{f,bind})/2} = t^{P} & (t < t_c) \\ t^{1/2} & (t > t_c) \end{cases} \qquad (3a)$$

Where,

$D_{f,bind}$ / $D_f$ = Fractal dimension of the surface (during binding step)

$t_c$ = Cross over value

The cross over value can be determined by using the relationship $r_c^2 \sim t_c$. Any value above $r_c$ (characteristic length) means that the self-similarity is lost and the surface may be considered homogeneous. Above the time $t_c$, the surface can be considered to be homogeneous and normal diffusion can be assumed present. For the reactions considered in this thesis, the value of $t_c$ is assumed not to have been reached and is arbitrary.

In the above equation the concentration of the product (analyte-receptor complex) on a solid fractal surface varies at two different time scales: (i) p = ½ at intermediate time scale, and (ii) with coefficient p = $(3 - D_{f,bind})/2$ at short time scales (Suleiman et al. 1991). The value of the coefficient p is not zero because of two factors; the improper diffusion and the heterogeneity. $D_{f,bind}$ is equal to two for a homogeneous surface. When the analyte in solution

views the receptor coated biosensor surface (fractal object) from a 'large distance', the coefficient p equals to half. During the binding process, the diffusion of the analyte from the solution to the surface of the receptor creates a depletion layer of width $(Đt)^{1/2}$, where Đ is the diffusion constant. This generates the fractal power law, $[\text{analyte.receptor}] \sim t^{(3 - D_{f,bind})/2}$ (Sadana et al. 2011).

The units for the binding coefficient $k_{bind}$ is $(pg)(mm)^{-2}(sec)^{(D_{f,bind} - 3)/2}$ and is not fixed as the time dependence factor in the unit varies depending on the fractal dimension derived during the binding phases, $D_{f,bind}$. In cases where there is a single fracal $k_{bind}$ and $k_{diss}$ may be referred to as k and $k_d$.

The fractal dimension is usually dependent on the receptor or analyte surface, but in this case it's dependent on the biosensor surface that is also the immobilizing surface. Li et al. (1995) showed that fractal surfaces could be formed by the active sites themselves. Including non-specific binding sites on the surface of the biosensor would also cause the fractal dimension to increase. All the factors stated above could be contributors to the variations in the binding coefficients and fractal dimensions obtained from the literature. It is therefore not accurate to conclude what the main influence on the fractal properties is.

3.1.2 Dissociation rate coefficient – The following equation describes the diffusion of the dissociated particle from the surface (complex coated surface) into the solution (Sadana et al. 2011):

$$(\text{analyte.receptor}) \begin{cases} - t^{(3-D_{f,diss})/2} & (t < t_{diss}) \\ - k_{diss}^{(3-D_{f,diss})/2} & \end{cases} \qquad (3b)$$

$D_{f,diss}$ = Fractal dimension of the surface (during dissociation step)

$t_{diss}$ = Start of the dissociation step

The dissociation step starts off after the maximum concentration of analyte-receptor on the surface has been reached. After this point, concentration decreases and hence dissociation occurs. The fractal dimension of the dissociation phase may or may not be equal to that of the binding phase, although theoretically they should match the difference could be as a result of numerous factors. The units for the rate of dissociation, $k_{diss}$ are the same as that of the binding coefficient, $k_{bind}$ i.e. $(pg)(mm)^{-2}(sec)^{(D_{f,diss}-3)/2}$. Like the units for the binding rate coefficient, the time dependency changes due to the change in the fractal dimension, $D_{f,diss}$.

3.2 Dual-Fractal Analysis

3.2.1 Binding rate coefficient – When a single fractal analysis is not adequate to describe the fit, dual fractals may be used. The concentration for the analyte-receptor complex for a dual fractal analysis is given by:

$$(\text{analyte.receptor}) \sim \begin{cases} t^{(3-D_{f1,bind})/2} = t^{P_1} & (t < t_1) \\ t^{(3-D_{f2,bind})/2} = t^{P_2} & (t_1 < t < t_2 = t_c) \\ t^{1/2} & (t > t_c) \end{cases} \qquad (3c)$$

At time $t = t_1$ is the start of the second fractal dimension, or in other words the point where the first fractal converges into the second one and is considered to be empirical and arbitrary. The cause for the variation in fractal dimension is as a result of the binding reaction being different from catalytic reactions. In the analyte-receptor binding, the surface of the biosensor portrays a changing fractal surface to the analyte in solution, whereas in that of a catalytic reaction the surface offers no changing fractals as long as there is no influence from external factors. The fractals on the analyte-receptor reactions are caused as a result of lack of 'binding' sites available as the reaction progresses, resulting in an increase in the degree of

heterogeneity on the surface of the biosensor. This is represented by dual fractal analysis of two degree of heterogeneity on the surface of the biosensor (Hutchison et al. 1995).

The application of a dual fractal analysis to the data analyzed is generally determined by whether a single fractal is adequate or not, which is done by observing the regression coefficient value ($r^2$). If the regression coefficient falls below 0.97 for a single fractal analysis, then a dual-fractal analysis is required to model the data. The binding rate coefficients of the dual fractal analysis, $k_1$ and $k_2$ have the same units as the single fractal analysis binding rate coefficient k.

3.2.1 Dissociation rate coefficient – The dissociation rate coefficient is given by:

$$(\text{analyte.receptor}) \sim \begin{cases} - t^{(3-D_{f1,diss})/2} & (t_{diss} < t < t_{d1}) \\ - t^{(3-D_{f2,diss})/2} & (t_{d1} < t < t_{d2}) \end{cases} \qquad (3d)$$

$D_{f,diss}$ = Fractal dimension of the surface (during dissociation step)

$t_{diss}$ = Start of the dissociation step

The dissociation step starts off after the maximum concentration of analyte-receptor on the surface has been reached. After this point, concentration decreases and hence dissociation occurs. The units for the rate of dissociation, $k_{d1}$ and $k_{d1}$ of the dual-fractal analysis have the same units i.e. $(pg)(mm)^{-2}(sec)^{(D_{f,d1} - 3)/2}$ and $(pg)(mm)^{-2}(sec)^{(D_{f,d1} - 3)/2}$ as that of the single fractal dissociation coefficient $k_d$. Like the units for the binding rate coefficient, the time dependency changes due to the change in the fractal dimension, $D_{f,d1}$ and $D_{f,d2}$.

Generally in an analysis that involves binding and dissociation phases, the affinity (K) can be calculated. The formula for calculating the affinity, is $K = k_{diss}/k_{bind}$ and is of upmost practical importance as it can help in determining various physical parameters on the

biosensor surface such as stability, regenerability and performance parameters. The units for the affinity are $(sec)^{[D_{f,diss}-D_{f,bind}]/2}$ and are applicable to both single and dual fractal analysis. The affinity calculated based on fractal analysis may have the same definition as that of the classical kinetics but differs in units due to the fact that the fractal affinity accounts for surface characteristics and the other does not. Hence, the two affinities cannot be fairly compared, as they are derived based on different systems and therefore the variation in results as compared to the literature (Sadana et al. 2011).

### 3.3 Triple-Fractal Analysis

When a dual-fractal analysis doesn't provide an adequate fit, a triple-fractal analysis may be applied to the model. One may easily extend both the single and dual-fractal analysis equations to describe the binding or dissociation kinetics exhibited by a triple fractal analysis. In extreme cases, n fractal dimensions may be present and the degree of heterogeneity, $D_f$, is changing continuously on the surface and needs to be represented by $D_{fi}$ where i = 1 – n. The same applies to the dissociation phase (Sadana et al. 2011).

The triple-fractal analysis can be described by the following equations:

$$(\text{analyte.receptor}) \sim \begin{cases} t^{(3-D_{f1,bind})/2} = t^{P}{}_{1} & (t < t_1) \\ t^{(3-D_{f2,bind})/2} = t^{P}{}_{2} & (t_1 < t < t_2) \\ t^{(3-D_{f3,bind})/2} = t^{P}{}_{3} & (t_2 < t < t_3 = t_c) \\ t^{1/2} & (t > t_c) \end{cases} \qquad (3e)$$

# CHAPTER 4

# RESULTS

A fractal analysis is applied to the data obtained for the different glucose biosensor readings from the literature. Fractal analysis is one of the ways to analyze the binding and dissociation kinetics occurring on the heterogeneous surfaces of the biosensor systems. Other ways include first-order reaction, saturation and no diffusion limitation cases, but these fail to include the heterogeneity that exists on the surface of the biosensor. The most common method used is the Langmuirian method for analyzing and modeling data, but this is only best used if one assumes the presence of discrete types of sites.

Lee et al. (1995) showed that the fractal approach has already been implemented to surface science i.e. reaction and adsorption processes. This approach not only provided a way to represent the morphology and different structures contained at the surface of reaction, but also develops optimal structures as a means for predictive approach. Another advantage of this approach is that it provides a lumped parameter(s) analysis of the diffusion-limited reaction, taking place on the heterogeneous surface, as it involves the complex analyte-receptor reaction that accounts for the fractal dimension and rate coefficient. This analysis helps in comparing different analyte-receptor biosensor systems.

In general to determine a fractal analysis, sufficient amount of data is required in order to construct a log-log plot. It is also beneficial to compare this plotted data to other kind of fits (exponential). In this thesis however, there will be no comparison as the degree of heterogeneity that exists on the surface of the biosensor is quantitative and plays an important

role on how the plot turns out. Hence there is some arbitrariness in the fractal model presented. The analysis in this thesis does not account for the nonselective adsorption of the analyte. The adsorption is solely dependent on surface availability and if it were to be accounted for in the analysis, it would lead to an increase in heterogeneity on the surface which would in turn lead to a higher fractal dimension value, since it is a direct measure of degree of heterogeneity on the surface of the biosensor (Knoblauch et al. 1999).

In general reaction orders obtained are higher than the first-order reactions, but if non-specific binding were to be included in the analysis it would lead to an increase in heterogeneity and a lower value of binding rate coefficient. A higher value of binding rate coefficient for the first-order reaction can be achieved by the elimination of the non-specific binding in the analysis. For reaction orders greater than one, a certain amount of heterogeneity is useful for the binding rate coefficient (Sadana et al. 1996). There is an optimum range influenced by steric factors that decides the incorporation of non-specific binding in the analysis. This means that in a certain range the influence of non-specific binding results in higher values of the binding coefficient for the same reaction order. In the case of the analysis of this thesis, a lower value of binding coefficient will be assumed incase of deletion of the non-specific binding.

The analysis performed in the past-utilized software provided by manufacturers of SPR biosensors to obtain affinity and rate coefficient values (Biacore AB, 2002). These models however did not take into account the heterogeneity present on the surface of the biosensor. The following analysis represents the heterogeneity observed on the surface of the biosensor with the help of the single, dual and triple fractal analysis.

The figures representing the fractal analysis of the data all consist the following key:

| | |
|---|---|
| Dashed line (----) | Single fractal Analysis |
| Continuous line (—) | Adequate fit (Single, Double or Triple fractal analysis) |
| Solid square (■) | Recorded data |

4.1 Common glucose sensor with a lead anode and platinum cathode dipped in electrolyte

Sienko et al. (2003) recorded the readings from a typical biosensor that contained typical oxygen electrodes, with both the cathode (Pt) and anode (Pb) structured so as they are immersed in 30% NaOH electrolyte. The sensor is placed in a buffer solution and stirred using a magnetic stirrer.

A regression analysis was performed on the data recorded by Sienko et al. (2003) on addition of (A) 2, (B) 4 and (C) 6 mM glucose to the sensor as shown in Figure 3. A single-fractal analysis is inadequate to describe the binding kinetics as can be seen from Figure 3 (represented by --- line). A dual-fractal analysis improves the fit but still has a low $r^2$ value. Due to the concentration of the analyte in solution, a triple-fractal analysis seemed to give a better fit and an acceptable $r^2$ value. Hence, all the concentrations required a triple fractal analysis to adequately describe the binding kinetics. The values for (a) the binding rate coefficient, k, for a single fractal analysis, (b) the binding rate coefficients, $k_1$, $k_2$ and $k_3$ for a triple-fractal analysis, (c) the fractal dimension, $D_f$, for binding for a single-fractal analysis, and (d) the fractal dimensions, $D_{f1}$, $D_{f2}$ and $D_{f3}$ for the binding for a triple fractal analysis are presented in Table 1. Since there is no dissociation phase occurring here, no affinity values are presented. A higher concentration of the receptors on the surface generally leads to a higher degree of heterogeneity because of all the enzyme active sites on the surface being saturated.

Figure 3a shows that the binding rate coefficient, $k_1$, increases with an increase in the fractal dimension, $D_{f1}$. The binding rate coefficient, $k_1$, is given by:

$$k_1 = (0.0045 \pm 0.00048)\, D_{f1}^{(0.48 \pm 0.32)}$$

The binding rate coefficient, $k_1$, in this case is slightly sensitive to the degree of heterogeneity on the surface of the biosensor as can be noted by the 0.48 order of dependence on the fractal dimension, $D_{f1}$.

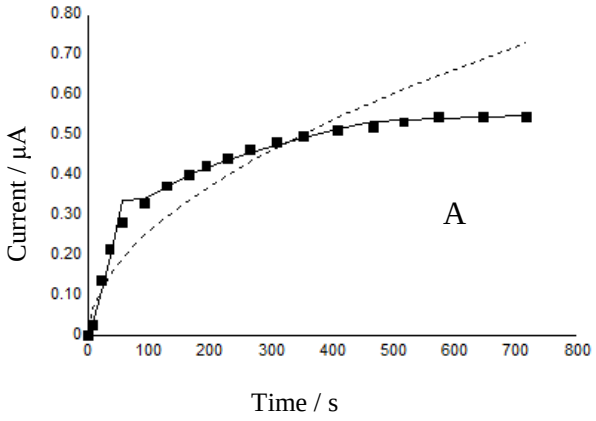


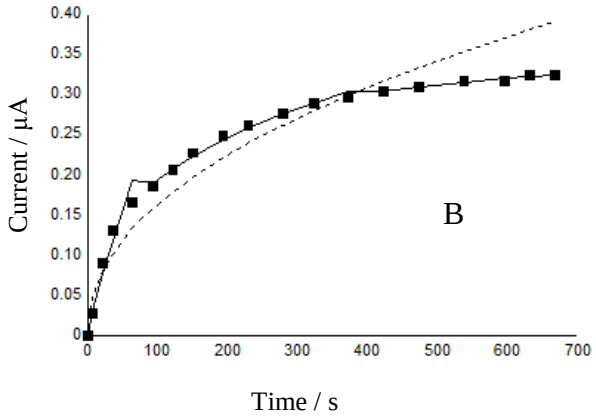


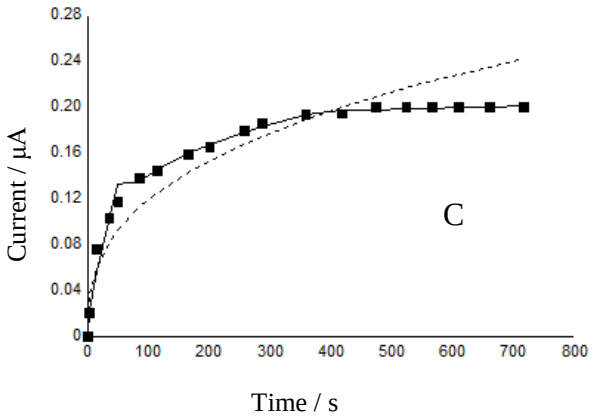


Figure 3: Binding of glucose molecules modeled on results based on a typical glucose sensor with a Pb anode and Pt cathode dipped in 30 % NaOH / KOH. (Sienko et al. 2003): (a) 6 mM (b) 4 mM (c) 2 mM

| Analyte/Receptor | k | $k_1$ | $k_2$ | $k_3$ | $D_f$ | $D_{f1}$ | $D_{f2}$ | $D_{f3}$ |
|---|---|---|---|---|---|---|---|---|
| A | 0.023 ± 0.008 | 0.003 ± 0.001 | 0.094 ± 0.002 | 0.347 ± 0.004 | 1.952 ± 0.113 | 0.708 ± 0.297 | 2.436 ± 0.022 | 2.862 ± 0.081 |
| B | 0.020 ± 0.004 | 0.006 ± 0.001 | 0.041 ± 0.001 | 0.129 ± 0.001 | 2.081 ± 0.076 | 1.325 ± 0.230 | 2.322 ± 0.029 | 2.715 ± 0.032 |
| C | 0.023 ± 0.005 | 0.009 ± 0.003 | 0.045 ± 0.001 | 0.154 ± 0.001 | 2.284 ± 0.070 | 1.640 ± 0.251 | 2.505 ± 0.020 | 2.919 ± 0.039 |

Table 1: Binding rate coefficients and Fractal dimensions of glucose molecules in solution to a typical glucose sensor with a Pb anode and Pt cathode dipped in 30 % NaOH / KOH. (Sienko et al. 2003): (A) 6 mM (B) 4 mM (C) 2 mM

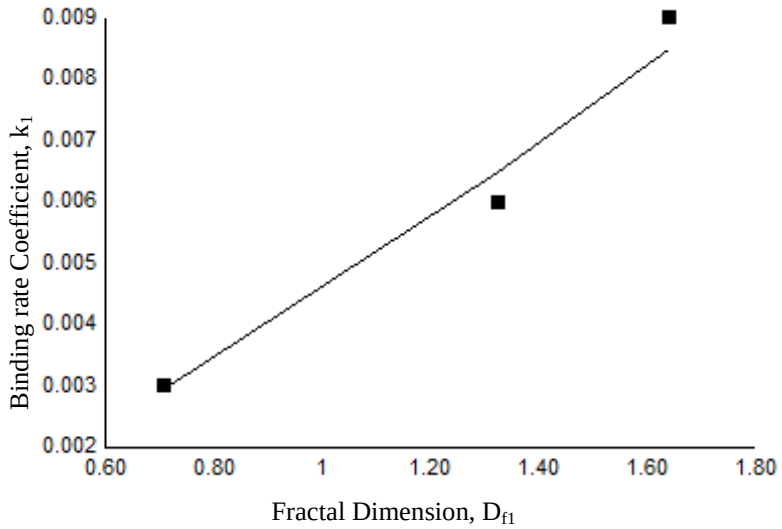


Figure 3a: Increase in the binding rate coefficient, $k_1$, with an increase in the fractal dimension for binding, $D_{f1}$.

As can be seen from Figure 3a, as the concentration of glucose increases, all the active sites on the surface of the biosensor get saturated, leading to a higher degree of heterogeneity on the surface. This saturation of active sites also changes the binding mechanism, eventually resulting in higher binding coefficients.

4.2 Glucose biosensor based on reagentless graphite-epoxy screen-printable composite

Galan-Vidal et al. (1997) developed an electrochemical sensing material made from graphite-epoxy composite to construct an amperometric transducer by using thick-film technology. They developed an optimized transducer using this graphite material for use in a glucose biosensor that measured the change in concentration of hydrogen peroxide produced. The screen-printable material was bulk modified with the addition of glucose oxidase and its purpose was to simplify the immobilization step on the transducer. They used three electrodes, a platinum counter electrode (Ingold), double junction Ag/AgCl reference electrode (Orion) with 0.1 M KCl solution and graphite-epoxy screen printing transducer as the working electrode. The analytical signal was at 1150 mV (Ag/AgCl) and the response of the sensor was linear for glucose concentration of 0.05 to 2.5 mM in a buffer solution of pH 7.0 with 0.1 M KCl and 0.1 M phosphate.

Figure 4 and 5 show the binding of the glucose molecule to the biosensor surface with the modified transducer by Galan-Vidal et al (1997). The glucose was added in 10 steps (Model A – J) at equal concentrations from 0 to 2.5 mM and at time intervals of approximately 30 seconds between each addition. A fractal analysis was carried out using Corel Quattro Pro X5 to model the data using the dual fractal equations (equation 3c) for the binding phase. A single fractal analysis was inadequate to describe the binding kinetics for each of the glucose concentrations; hence a dual-fractal analysis was applied.

The values for (a) the binding rate coefficient, k, for a single fractal analysis, (b) the binding rate coefficients, $k_1$ and $k_2$ for a dual-fractal analysis, (c) the fractal dimension, $D_f$, for binding for a single-fractal analysis, and (d) the fractal dimensions, $D_{f1}$ and $D_{f2}$ for the binding for a dual-fractal analysis are presented in Table 2.

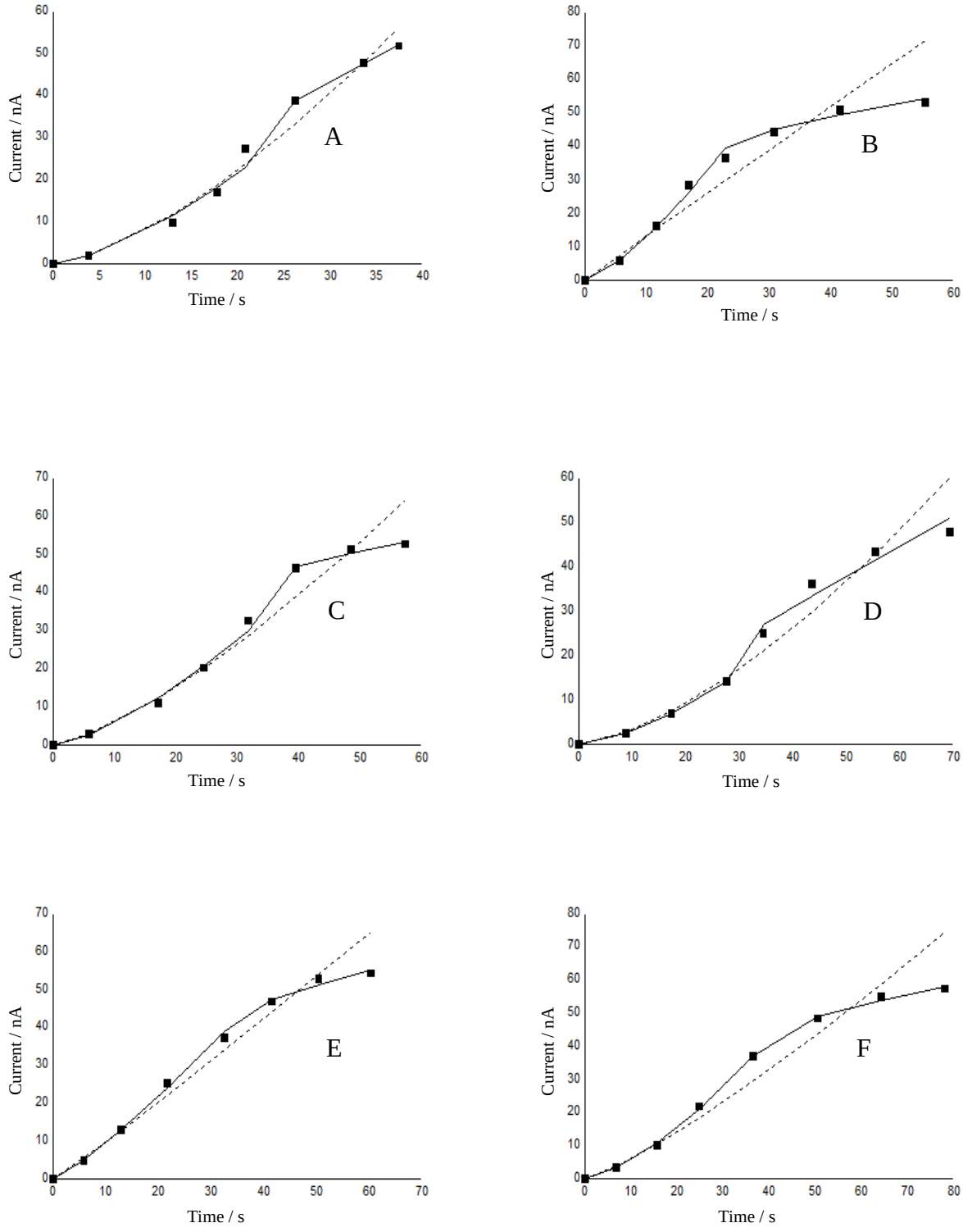


Figure 4: Binding of Glucose molecules in solution by linear addition of 0 to 2.4 mM at time interval of 30 seconds. Working solution: 0.1 M phosphate and 0.1 M KCl buffer solution at pH 7.0 and applied potential of 1150 mV vs Ag/AgCl (Galan-Vidal et al. 1997) Model A – F

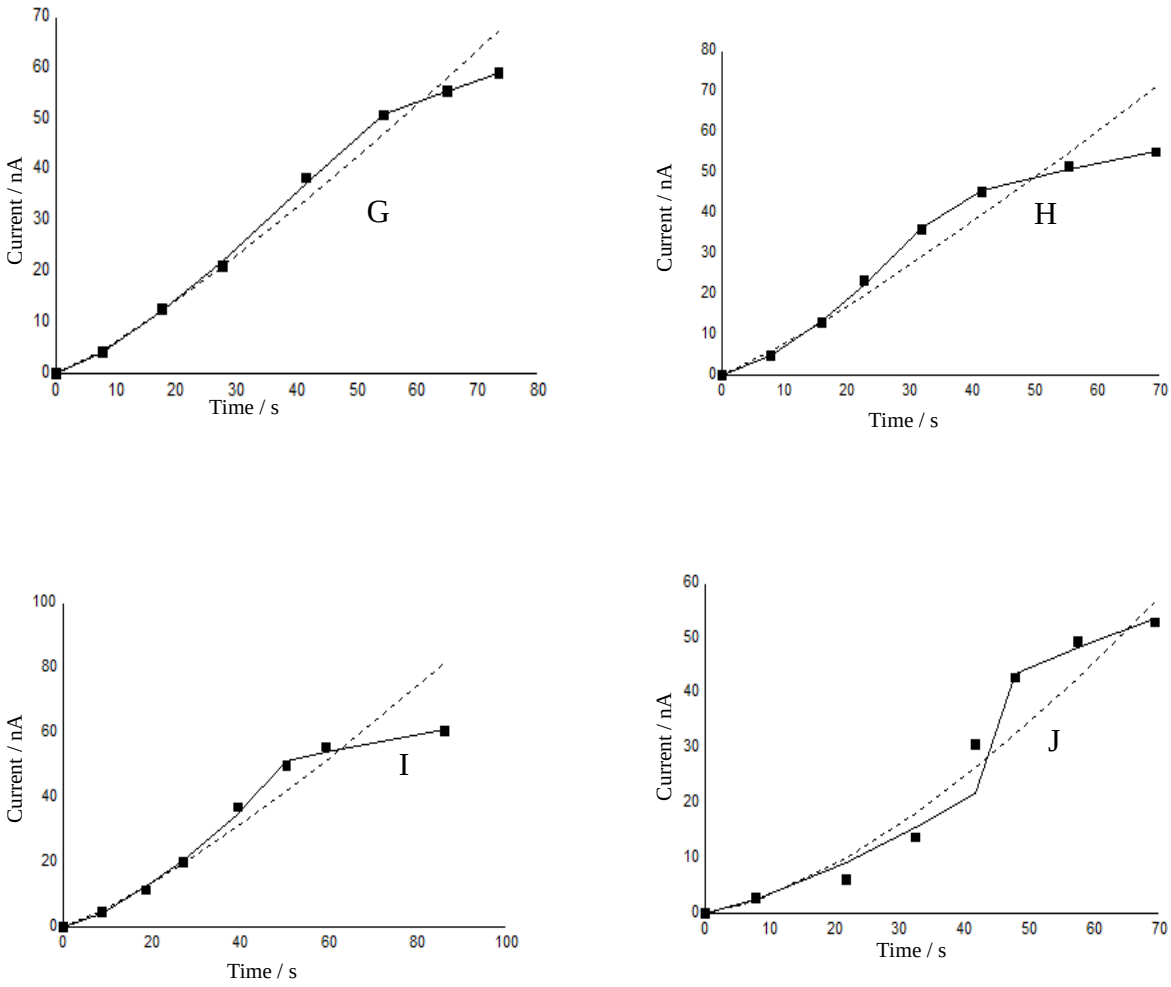


Figure 5: Binding of Glucose molecules in solution by linear addition of 0 to 2.4 mM at time interval of 30 seconds. Working solution: 0.1 M phosphate and 0.1 M KCl buffer solution at pH 7.0 and applied potential of 1150 mV vs Ag/AgCl (Galan-Vidal et al. 1997) Model G – J

| Analyte/Receptor | k | $k_1$ | $k_2$ | $D_f$ | $D_{f1}$ | $D_{f2}$ |
|---|---|---|---|---|---|---|
| A | 0.273 ± 0.040 | 0.280 ± 0.053 | 2.641 ± 0.011 | 0.061 ± 0.144 | 0.098 ± 0.264 | 1.356 ± 0.032 |
| B | 1.360 ± 0.361 | 0.560 ± 0.048 | 15.516 ± 0.615 | 1.027 ± 0.246 | 0.282 ± 0.157 | 2.378 ± 0.186 |
| C | 0.260 ± 0.040 | 0.226 ± 0.027 | 12.962 ± 0.294 | 0.279 ± 0.149 | 0.178 ± 0.173 | 2.303 ± 0.171 |
| D | 0.102 ± 0.018 | 0.010 ± 0.000 | 1.066 ± 0.102 | na | 0.012 ± 0.000 | 1.177 ± 0.352 |
| E | 0.376 ± 0.079 | 0.206 ± 0.011 | 10.410 ± 0.304 | 0.575 ± 0.780 | 0.117 ± 0.086 | 2.211 ± 0.185 |
| F | 0.341 ± 0.068 | 0.217 ± 0.018 | 14.059 ± 0.565 | 0.544 ± 0.193 | 0.237 ± 0.143 | 2.343 ± 0.202 |
| G | 0.392 ± 0.039 | 0.304 ± 0.013 | 6.872 ± 0.009 | 0.606 ± 0.096 | 0.419 ± 0.069 | 2.000 ± 0.012 |
| H | 0.852 ± 0.113 | 0.613 ± 0.030 | 10.632 ± 0.376 | 0.883 ± 0.122 | 0.615 ± 0.075 | 2.197 ± 0.113 |
| I | 0.546 ± 0.118 | 0.249 ± 0.009 | 10.704 ± 0.151 | 0.703 ± 0.211 | 0.119 ± 0.067 | 2.225 ± 0.077 |
| J | 0.103 ± 0.038 | 0.159 ± 0.078 | 4.900 ± 0.152 | 0.022 ± 0.348 | 0.360 ± 0.629 | 1.872 ± 0.232 |

Table 2: Binding rate coefficients and Fractal dimensions of glucose molecules in solution to a sensor with working solution: 0.1 M phosphate and 0.1 M KCl buffer solution at pH 7.0 and applied potential of 1150 mV vs Ag/AgCl. Glucose concentration added linearly from 0 to 2.4 mM at time interval of 30 seconds (Galan-Vidal et al. 1997)

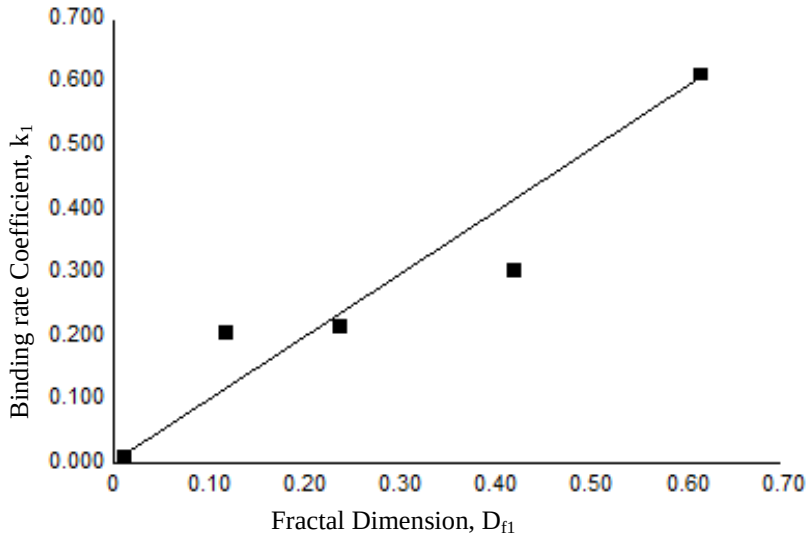


Figure 4-5a: Increase in the binding rate coefficient, $k_1$, with an increase in the fractal dimension for binding, $D_{f1}$.

Figure 4-5a shows that the binding rate coefficient, $k_1$, increases with an increase in the fractal dimension, $D_{f1}$ for models D-H. The binding rate coefficient, $k_1$, is given by:

$$k_1 = (0.98 \pm 0.47)\, D_{f1}^{(1.01 \pm 0.25)}$$

The binding rate coefficient, $k_1$, in this case is moderately sensitive to the degree of heterogeneity on the surface of the biosensor as can be noted by the 1.01 order of dependence on the fractal dimension, $D_{f1}$. Model D-H exhibited the increase in binding coefficient, $k_1$, with an increase in the fractal dimension, $D_{f1}$. As can be observed from the models in Figure 4 and Figure 5, these exhibit an adequate fit when the dual-fractal analysis is applied, hence resulting in the increase with the fractal dimension as binding coefficient increases due to increase in heterogeneity of the surface of the biosensor.

4.3 Glucose biosensor based on an inhibition enzyme incorporating an electropolymerized aniline membrane and ferrocene as electron transfer mediator

Zeng et al. (2004) developed a biosensor with inhibited enzyme glucose oxidase. They prepared an electropolymerized aniline membrane on which they cross-linked the glucose oxidase enzyme by glutaraldehyde and used a platinum electrode with ferrocene as an electron transfer agent. Cross-linkage is one of the ideal cases of fabricating sensor membrane as stated by Sienko et al. (2003). They inhibited the enzyme on the sensor with chromium (VI) to decrease its sensitivity to glucose molecule. This resulted in the enzyme membrane completely reactivating after inhibition and retaining close to 90% of its activity for more than forty days.

The author indicated improved electron transfer of the redox reaction by trapping ferrocene in the polymer membrane as an electron transfer mediator; this in turn increased glucose sensitivity of the sensor at optimum voltage of +0.7V. The buffer solution used is phosphate buffer with a pH 6.24.

Figure 6 and 7 show the binding of the glucose molecule to the inhibition-based enzyme biosensor surface. The glucose was added in varying intervals of time, each approximately 500 seconds apart and in concentrations of (A) 2.5, (B) 5, (C) 7.5, (D) 10, (E) 12.5, (F) 15, (G) 17.5, (H) 20 AND (I) 22.5 mM. A fractal analysis was carried out to model the data using the fractal equations for the binding phase. A single fractal analysis was inadequate to describe the binding kinetics for each of the glucose concentrations; hence a dual-fractal analysis was applied.

The values for (a) the binding rate coefficient, k, for a single fractal analysis, (b) the binding rate coefficients, $k_1$ and $k_2$ for a dual-fractal analysis, (c) the fractal dimension, $D_f$, for binding for a single-fractal analysis, and (d) the fractal dimensions, $D_{f1}$ and $D_{f2}$ for the binding for a dual-fractal analysis are presented in Table 3.

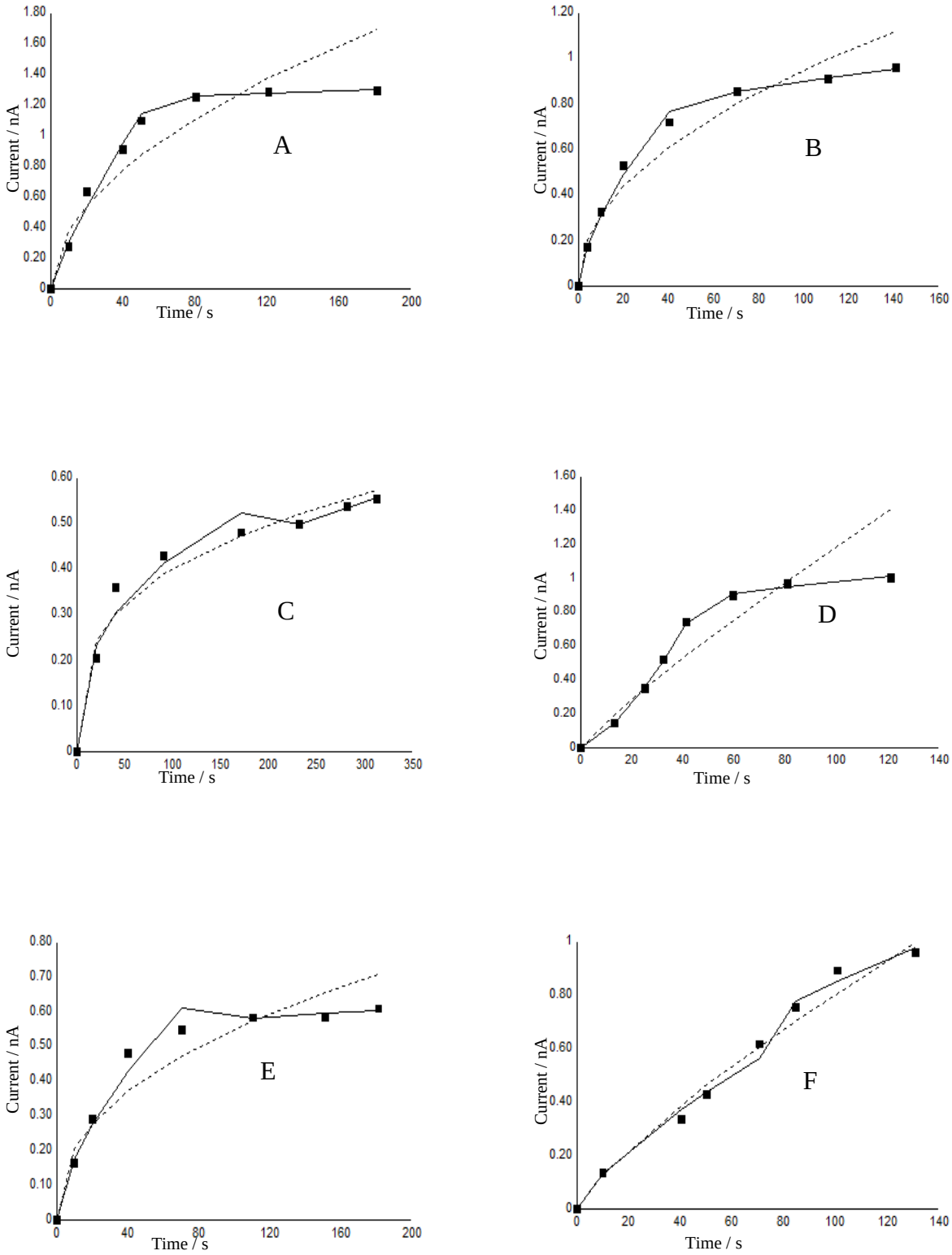


Figure 6: Binding of different concentrations of glucose molecules (in mM) to receptor in solution with phosphate buffer (pH 6.24) measured by amperometry at + 0.7 V. (Zeng et al. 2004): (a) 2.5 (b) 5 (c) 7.5 (d) 10 (e) 12.5 (f) 15

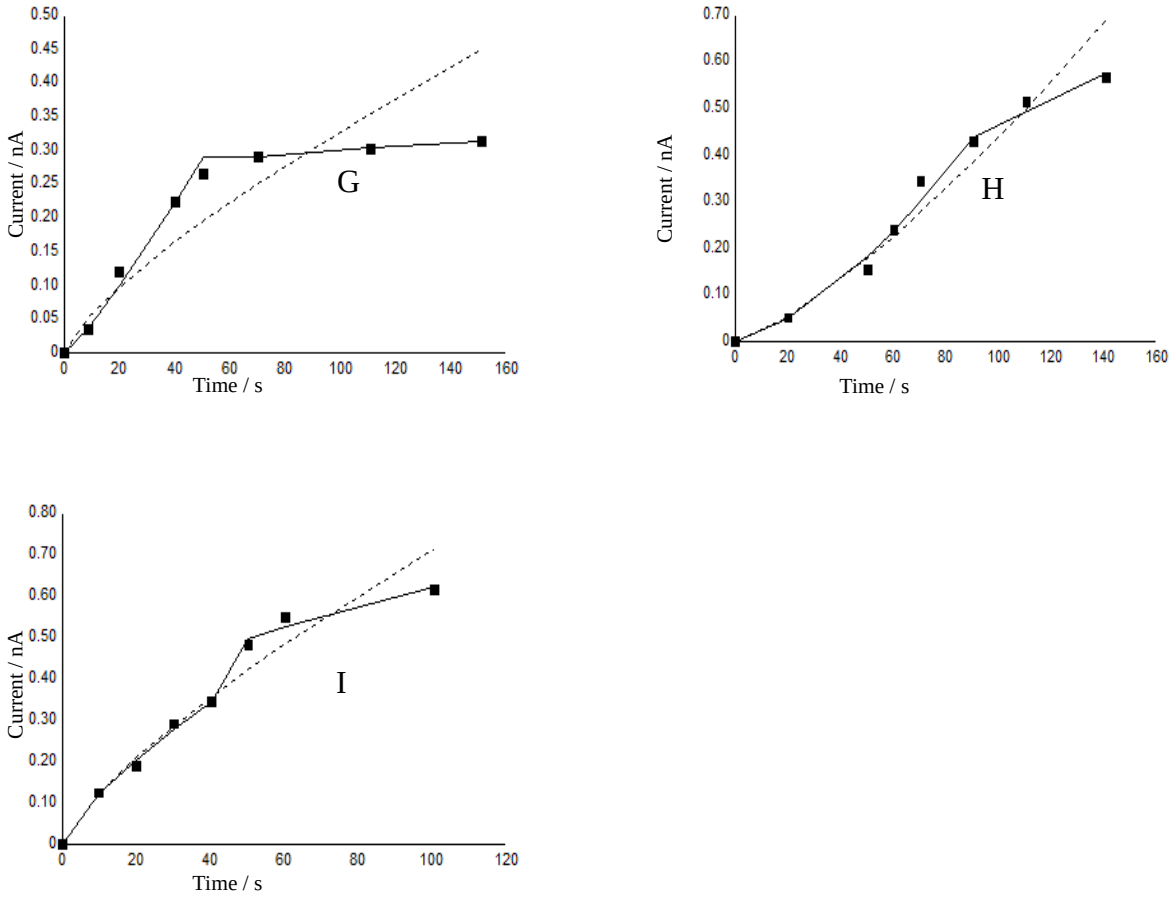


Figure 7: Binding of different concentrations of glucose molecules (in mM) to receptor in solution with phosphate buffer (pH 6.24) measured by amperometry at + 0.7 V. (Zeng et al. 2004): (g) 17.5 (h) 20 (i) 22.5

| Analyte/Receptor | k | $k_1$ | $k_2$ | $D_f$ | $D_{f1}$ | $D_{f2}$ |
|---|---|---|---|---|---|---|
| A | 0.115 ± 0.032 | 0.044 ± 0.007 | 1.045 ± 0.009 | 1.965 ± 0.197 | 1.345 ± 0.228 | 2.917 ± 0.029 |
| B | 0.104 ± 0.018 | 0.072 ± 0.006 | 0.433 ± 0.005 | 2.040 ± 0.101 | 1.725 ± 0.089 | 2.681 ± 0.051 |
| C | 0.096 ± 0.012 | 0.076 ± 0.014 | 0.067 ± 0.000 | 2.378 ± 0.094 | 2.249 ± 0.204 | 2.266 ± 0.022 |
| D | 0.001 ± 0.000 | 0.001 ± 0.000 | 0.027 ± 0.001 | 0.381 ± 0.200 | 0.106 ± 0.332 | 1.759 ± 0.293 |
| E | 0.010 ± 0.004 | 0.003 ± 0.001 | 0.194 ± 0.001 | 1.480 ± 0.286 | 0.646 ± 0.253 | 2.811 ± 0.018 |
| F | 0.021 ± 0.003 | 0.022 ± 0.001 | 0.138 ± 0.008 | 1.481 ± 0.125 | 1.500 ± 0.125 | 2.348 ± 0.212 |
| G | 0.020 ± 0.002 | 0.024 ± 0.003 | 0.073 ± 0.004 | 1.401 ± 0.094 | 1.514 ± 0.137 | 1.938 ± 0.370 |
| H | 0.076 ± 0.016 | 0.040 ± 0.006 | 0.397 ± 0.007 | 2.142 ± 0.142 | 1.725 ± 0.178 | 2.840 ± 0.102 |
| I | 0.021 ± 0.006 | 0.004 ± 0.000 | 0.496 ± 0.011 | 1.239 ± 0.297 | 0.160 ± 0.068 | 2.704 ± 0.087 |

Table 3: Binding rate coefficients and Fractal dimensions of glucose molecules (mM) to receptor in solution with phosphate buffer (pH 6.24) measured by amperometry at + 0.7 V. (Zeng et al. 2004): (A) 2.5 (B) 5 (C) 7.5 (D) 10 (E) 12.5 (F) 15 (G) 17.5 (H) 20 (I) 22.5

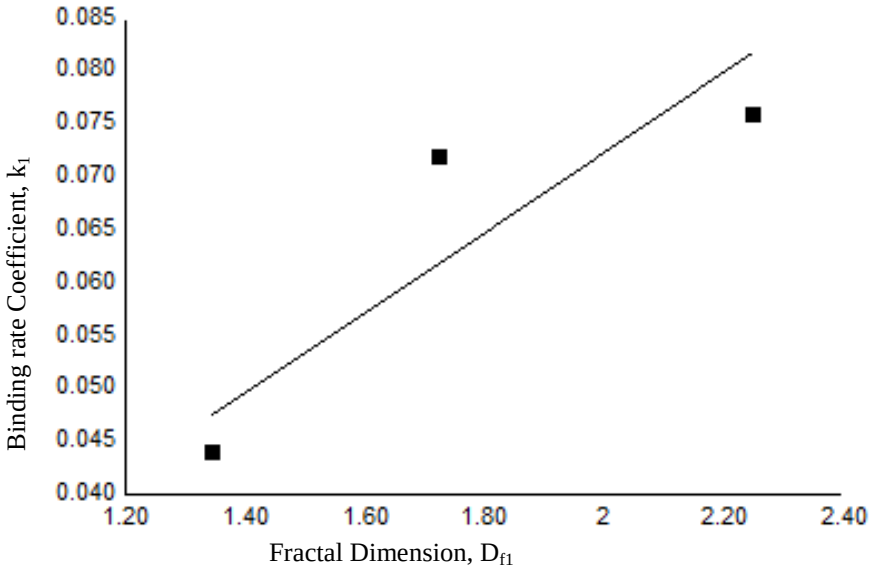


Figure 6a: Increase in the binding rate coefficient, $k_1$, with an increase in the fractal dimension for binding, $D_{f1}$.

Figure 6a shows that the binding rate coefficient, $k_1$, increases with an increase in the fractal dimension, $D_{f1}$ for models A-C. The binding rate coefficient, $k_1$, is given by:

$$k_1 = (0.035 \pm 0.007)\, D_{f1}^{(0.89 \pm 0.02)}$$

The binding rate coefficient, $k_1$, in this case is moderately sensitive to the degree of heterogeneity on the surface of the biosensor as can be noted by the 0.89 order of dependence on the fractal dimension, $D_{f1}$.

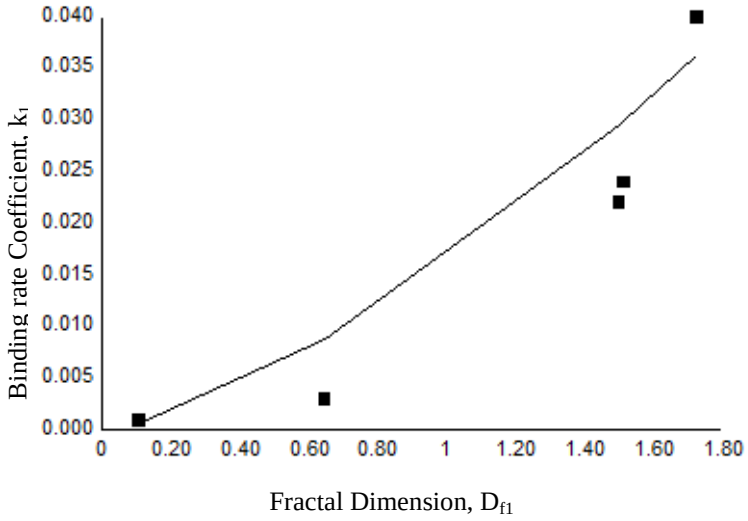


Figure 6-7a: Increase in the binding rate coefficient, $k_1$, with an increase in the fractal dimension for binding, $D_{f1}$.

Figure 6-7a shows that the binding rate coefficient, $k_1$, increases with an increase in the fractal dimension, $D_{f1}$ for models D-H. The binding rate coefficient, $k_1$, is given by:

$$k_1 = (0.016 \pm 0.015)\, D_{f1}^{(0.12 \pm 0.50)}$$

The binding rate coefficient, $k_1$, in this case is moderately sensitive to the degree of heterogeneity on the surface of the biosensor as can be noted by the 0.12 order of dependence on the fractal dimension, $D_{f1}$.

Zeng et al. (2004) further went ahead and ran another set of tests with 2.25 mM glucose in solution, and then cleaned it out and restarted the voltage with the same concentration. A regression analysis was performed on this data and is shown in Figure 8. A single-fractal analysis is inadequate to describe the binding kinetics as can be seen from Figure 8 (represented by --- line). A dual-fractal analysis improves the fit but still has a low $r^2$ value. Due to the concentration of the analyte in solution, a triple-fractal analysis seemed to

give a better fit and an acceptable $r^2$ value. Hence, all the concentrations required a triple fractal analysis to adequately describe the binding kinetics. The values for (a) the binding rate coefficient, k, for a single fractal analysis, (b) the binding rate coefficients, $k_1$, $k_2$ and $k_3$ for a triple-fractal analysis, (c) the fractal dimension, $D_f$, for binding for a single-fractal analysis, and (d) the fractal dimensions, $D_{f1}$, $D_{f2}$ and $D_{f3}$ for the binding for a triple fractal analysis are presented in Table 4. Since there is no dissociation phase occurring here, no affinity values are presented. A higher concentration of the receptors on the surface generally leads to a higher degree of heterogeneity because of all the enzyme active sites on the surface being saturated.

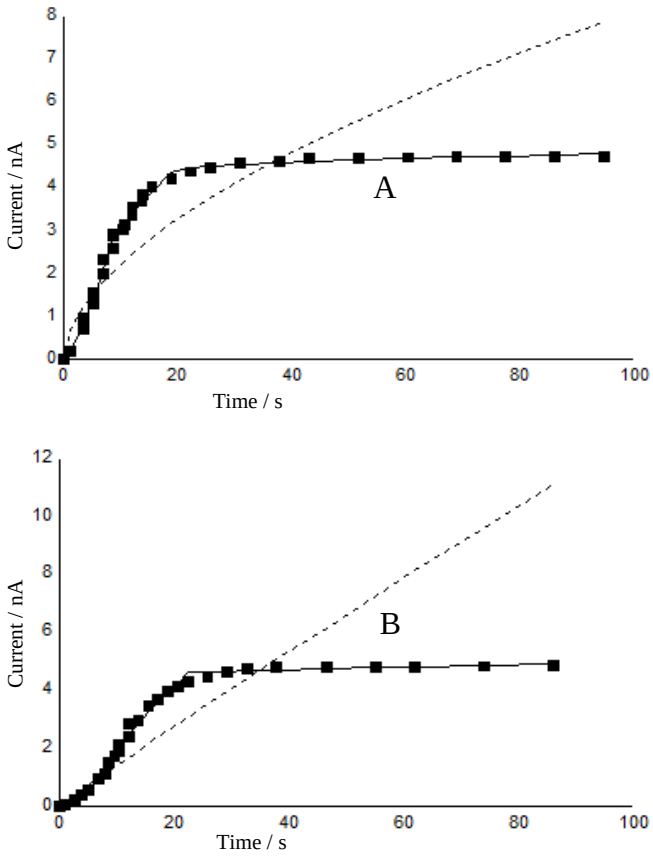


Figure 8: Binding of 2.25mM glucose molecules to receptor in solution. First run (a) Amperometric measurement in acetate buffer (pH 2.55) at + 0.7V and second run (b) immerse electrodes in phosphate buffer (pH 7.0) and restart current in acetate buffer (pH 2.55) followed by 2.25mM glucose addition. (Zeng et al. 2004)

| Analyte/Receptor | k | $k_1$ | $k_2$ | $k_3$ | $D_f$ | $D_{f1}$ | $D_{f2}$ | $D_{f3}$ |
|---|---|---|---|---|---|---|---|---|
| A | 0.897 ± 0.292 | 0.137 ± 0.016 | 0.907 ± 0.029 | 3.833 ± 0.043 | 1.874 0.138 | 0.181 ±0.144 | 1.933 ± 0.083 | 2.903 ± 0.014 |
| B | 0.242 ±0.086 | 0.058 ± 0.006 | 0.215 ± 0.017 | 3.957 ± 0.068 | 1.085 ± 0.166 | 0.081 ± 0.106 | 1.027 ± 0.179 | 2.905 ± 0.028 |

Table 4: Binding rate coefficients and Fractal dimensions of 2.25mM glucose molecules to receptor in solution. First run (A) Amperometric measurement in acetate buffer (pH 2.55) at + 0.7V and second run (B) immerse electrodes in phosphate buffer (pH 7.0) and resume current in acetate buffer (pH 2.55) followed by 2.25mM glucose addition. (Zeng et al. 2004)

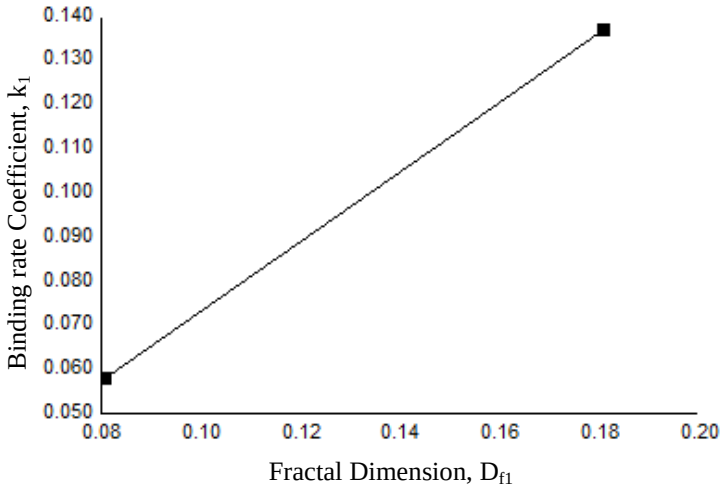


Figure 8a: Increase in the binding rate coefficient, $k_1$, with an increase in the fractal dimension for binding, $D_{f1}$.

The figure above (Figure 8a) shows that the binding rate coefficient, $k_1$, increases with an increase in the fractal dimension, $D_{f1}$. The binding rate coefficient, $k_1$, is given by:

$$k_1 = (0.852 \pm \text{n.a})\, D_{f1}^{(0.86 \pm \text{n.a})}$$

The binding rate coefficient, $k_1$, in this case is moderately sensitive to the degree of heterogeneity on the surface of the biosensor as can be noted by the 0.86 order of dependence on the fractal dimension, $D_{f1}$.

## 4.4 Glucose biosensor based on a single-supply embedded telemetry system for amperometric applications

Serra et al. (2007) presented an embedded telemetry system for amperometric applications of biosensors. They evaluated the system using a platinum (Pt) amperometric glucose biosensor. They prepared a glucose sensor based on the Poly-o-PD model by Lowry et al. (1998). The modified sensor was immersed in a cell filled with 5 ml of nitrogenated PBS containing the o-phenylenediamine monomer in nitrogen atmosphere. The auxiliary and reference electrodes used were a 50 mm platinum wire and an Ag/AgCl electrode. This sensor bundled with the single-supply embedded telemetry system exhibited classical Michaelis-Menten kinetics ($r^2$=0.9885) with better linearity at lower concentrations of glucose ($r^2$=0.9913). The sensor was stabilized in PBS at room temperature.

Figures 9 and 10 show the binding and dissociation of the glucose molecule to the biosensor surface. The glucose was added in varying intervals of time in concentrations of (A) 0.2, (B) 0.4, (C) 0.6, (D) 1, (E) 2, (F) 10, (G) 20, (H) 60, (I) 100 and (I) 140 mM. A fractal analysis was carried out to model the data using the fractal equations for the binding and dissociation phases. A single fractal analysis was inadequate to describe the binding kinetics for each of the glucose concentrations; hence a dual-fractal analysis was applied. Since the concentrations of models A and B exhibit a “convex” nature close to the start of the dissociation phase, their dissociation fractal dimension, $D_{fd}$, values are estimated to be zero.

The values for (a) the binding rate coefficient, k, for a single fractal analysis, (b) the binding rate coefficients, $k_1$ and $k_2$ for a dual-fractal analysis, (c) the dissociation rate coefficient, kd, for a single-fractal analysis, (d) the fractal dimension, $D_f$, for binding for a single-fractal analysis, (e) the fractal dimensions, $D_{f1}$ and $D_{f2}$ for the binding for a dual-fractal analysis, and (f) the fractal dimension, $D_{fd}$ for the dissociation for a single-fractal analysis are presented in Table 5.

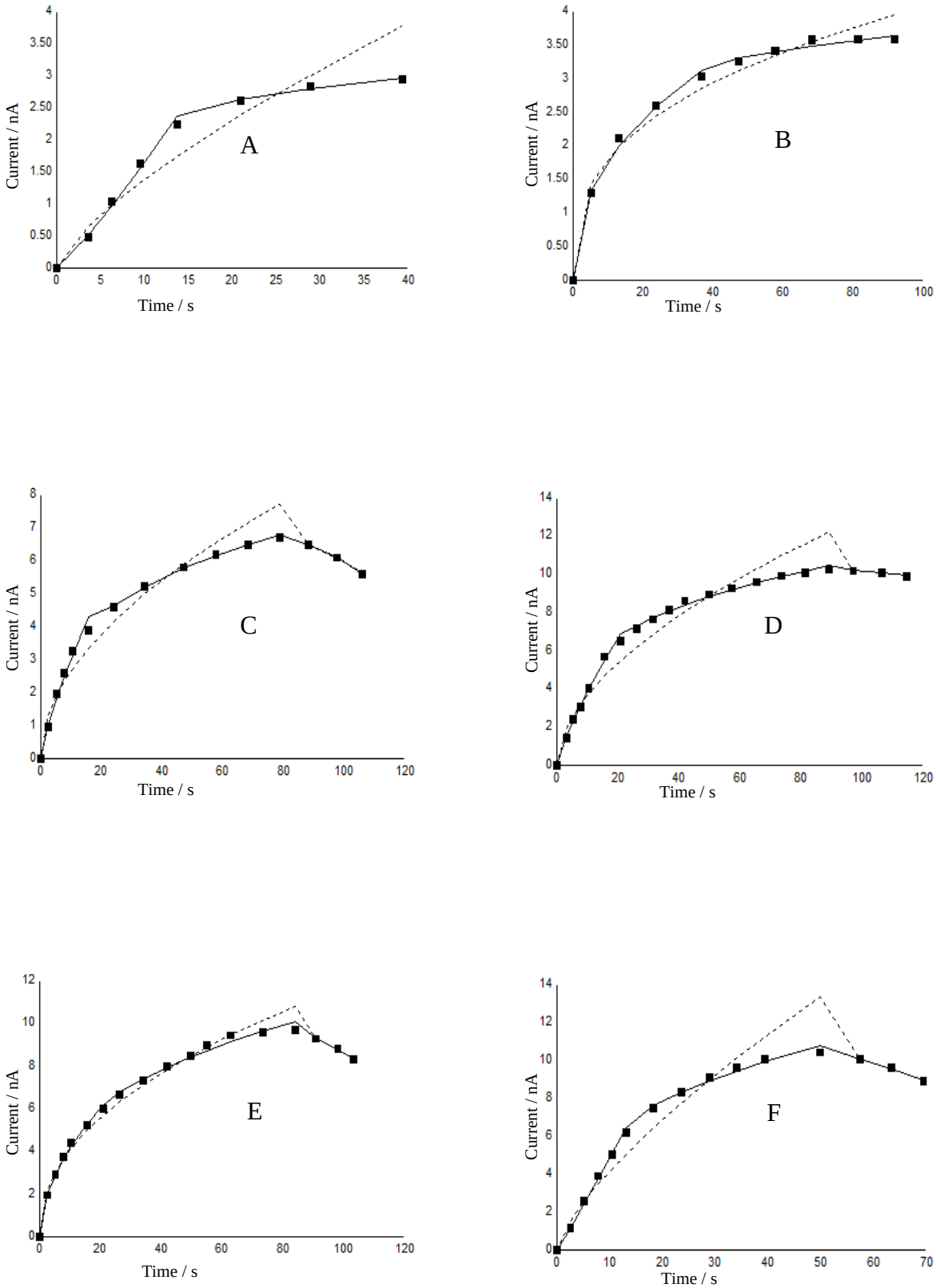


Figure 9: Binding and dissociation of different concentrations of glucose molecules (mM) in solution to receptor with a +700 mV potential applied to a Poly-o-PD based biosensor. (Serra et al. 2007): (a) 0.2 (b) 0.4 (c) 0.6 (d) 1 (e) 2 (f) 10

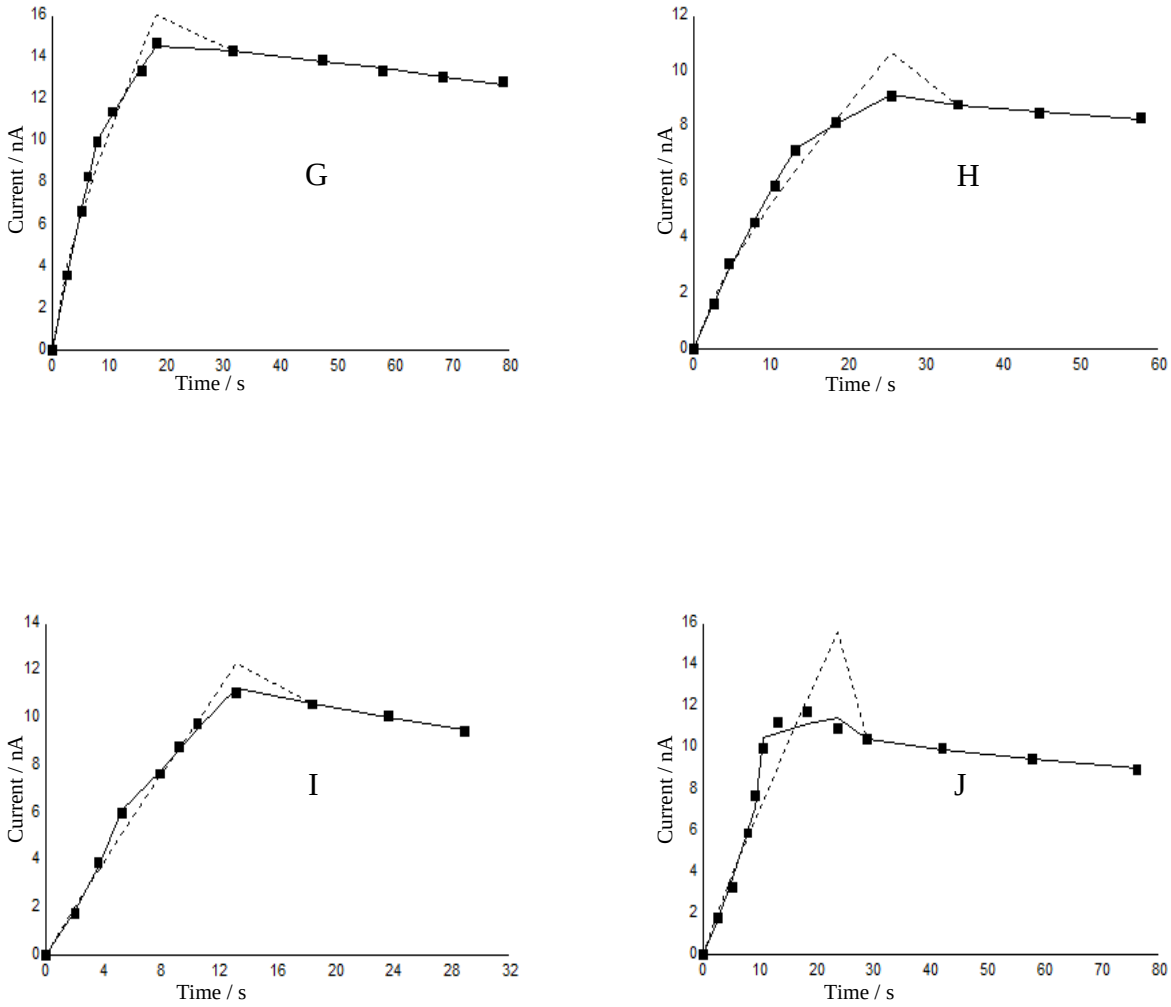


Figure 10: Binding and dissociation of different concentrations of glucose molecules (mM) in solution to receptor with a +700 mV potential applied to a Poly-o-PD based biosensor. (Serra et al. 2007): (g) 20 (h) 60 (i) 100 (j) 140

| Analyte/Receptor | k | $k_1$ | $k_2$ | $k_d$ | $D_f$ | $D_{f1}$ | $D_{f2}$ | $D_{fd}$ |
|---|---|---|---|---|---|---|---|---|
| A | 0.254 ± 0.066 | 0.118 ± 0.011 | 1.451 ± 0.030 | na | 1.530 ± 0.221 | 0.709 ± 0.173 | 2.610 ± 0.091 | na |
| B | 0.803 ± 0.060 | 0.653 ± 0.034 | 1.876 ± 0.038 | na | 2.296 ± 0.054 | 2.130 ± 0.070 | 2.706 ± 0.076 | na |
| C | 0.801 ± 0.133 | 0.485 ± 0.047 | 1.664 ± 0.014 | 0.009 ± 0.000 | 1.964 ± 0.086 | 1.418 ± 0.135 | 2.356 ± 0.017 | 0.070 ±0.136 |
| D | 1.013 ± 0.151 | 0.604 ± 0.037 | 2.826 ± 0.047 | 0.003 ± 0.001 | 1.891 ± 0.070 | 1.400 ± 0.077 | 2.417 ± 0.026 | 0.119 ± 0.428 |
| E | 1.398 ± 0.084 | 1.189 ± 0.036 | 2.197 ± 0.054 | 0.047 ± 0.002 | 2.077 ± 0.031 | 1.917 ± 0.036 | 2.312 ± 0.047 | 0.729 ± 0.137 |
| F | 0.771 ± 0.150 | 0.432 ± 0.023 | 2.811 ± 0.071 | 0.019 ± 0.001 | 1.540 ± 0.122 | 0.901 ± 0.081 | 2.313 ± 0.062 | 0.069 ± 0.143 |
| G | 2.055 ± 0.231 | 1.429 ± 0.056 | 3.969 ± 0.055 | 0.017 ± 0.001 | 1.598 ± 0.130 | 1.107 ± 0.118 | 2.110 ± 0.041 | 0.676 ± 0.130 |
| H | 0.898 ± 0.114 | 0.711 ± 0.051 | 2.837 ± 0.015 | 0.075 ± 0.009 | 1.474 ± 0.123 | 1.186 ± 0.130 | 2.279 ± 0.022 | 1.593 ± 0.239 |
| I | 1.043 ± 0.126 | 0.729 ± 0.023 | 1.760 ± 0.044 | 0.080 ± 0.004 | 1.081 ± 0.141 | 0.435 ± 0.091 | 1.559 ± 0.132 | 0.831 ± 0.137 |
| J | 0.834 ± 0.225 | 0.557 ± 0.070 | 7.986 ± 0.580 | 0.177 ± 0.006 | 1.148 ± 0.259 | 0.711 ± 0.244 | 2.772 ± 0.226 | 1.802 ± 0.041 |

Table 5: Binding and dissociation rate coefficients and Fractal dimensions of different concentrations of glucose molecules (mM) to receptor in solution with a +700 mV potential applied to a Poly-o-PD based biosensor. (Serra et al. 2007): (A) 0.2 (B) 0.4 (C) 0.6 (D) 1 (E) 2 (F) 10 (G) 20 (H) 60 (I) 100 (J) 140

4.5 Glucose biosensor based on immobilized enzyme on $NdPO_4$ nanoparticles on glassy carbon electrodes

Sheng et al. (2009) achieved the electrochemistry of glucose oxidase enzyme immobilized on a composite matrix based on $NdPO_4$ nanoparticles and chitosan (CHIT), underlying on a glassy carbon electrode. They measured the peak redox reactions exhibited by these modified electrodes using a cyclic voltammetry process in an air deprived buffer solution, which showed expected results, hence confirming the immobilization of the enzyme on the composite film. They indicated a linear dynamic range for detection of glucose from 0.15 – 10 mM concentration and exhibited a correlation coefficient ($r^2$) of 0.99. The authors then proceeded to calculate the Michaelis-Menten constant, whose results showed that there was a higher affinity of the enzyme-substrate achieved.

The immobilized enzyme retained its bioactivity and the proposed biosensor catalyzed the reduction of dissolved oxygen as stated. They indicated the use of this sensor for detection of glucose in human plasma, as it was stable and efficient to exclude interference from uric and ascorbic acid, hence offering a more selective and sensitive glucose biosensor.

Figures 11, 12 and 13 show the binding and dissociation of the glucose molecule to the modified biosensor surface. The glucose was added in incrementing intervals of time in concentrations of (A) 10, (B) 33, (C) 100, and (D) >100 μl 150 mM. A fractal analysis was carried out to model each of the peaks observed after addition of the stated glucose concentrations using the fractal equations for the binding and dissociation phases. A single fractal analysis was inadequate to describe the binding kinetics for each of the glucose concentrations; hence a dual-fractal analysis was applied. Since the concentrations of models A1 – A4 exhibit a “convex” nature close to the start of the dissociation phase, their dissociation fractal dimension, $D_{fd}$, values are estimated to be zero.

The values for (a) the binding rate coefficient, k, for a single fractal analysis, (b) the binding rate coefficients, $k_1$ and $k_2$ for a dual-fractal analysis, (c) the dissociation rate coefficient, kd, for a single-fractal analysis, (d) the fractal dimension, $D_f$, for binding for a single-fractal analysis, (e) the fractal dimensions, $D_{f1}$ and $D_{f2}$ for the binding for a dual-fractal analysis, and (f) the fractal dimension, $D_{fd}$ for the dissociation for a single-fractal analysis are presented in Table 6.

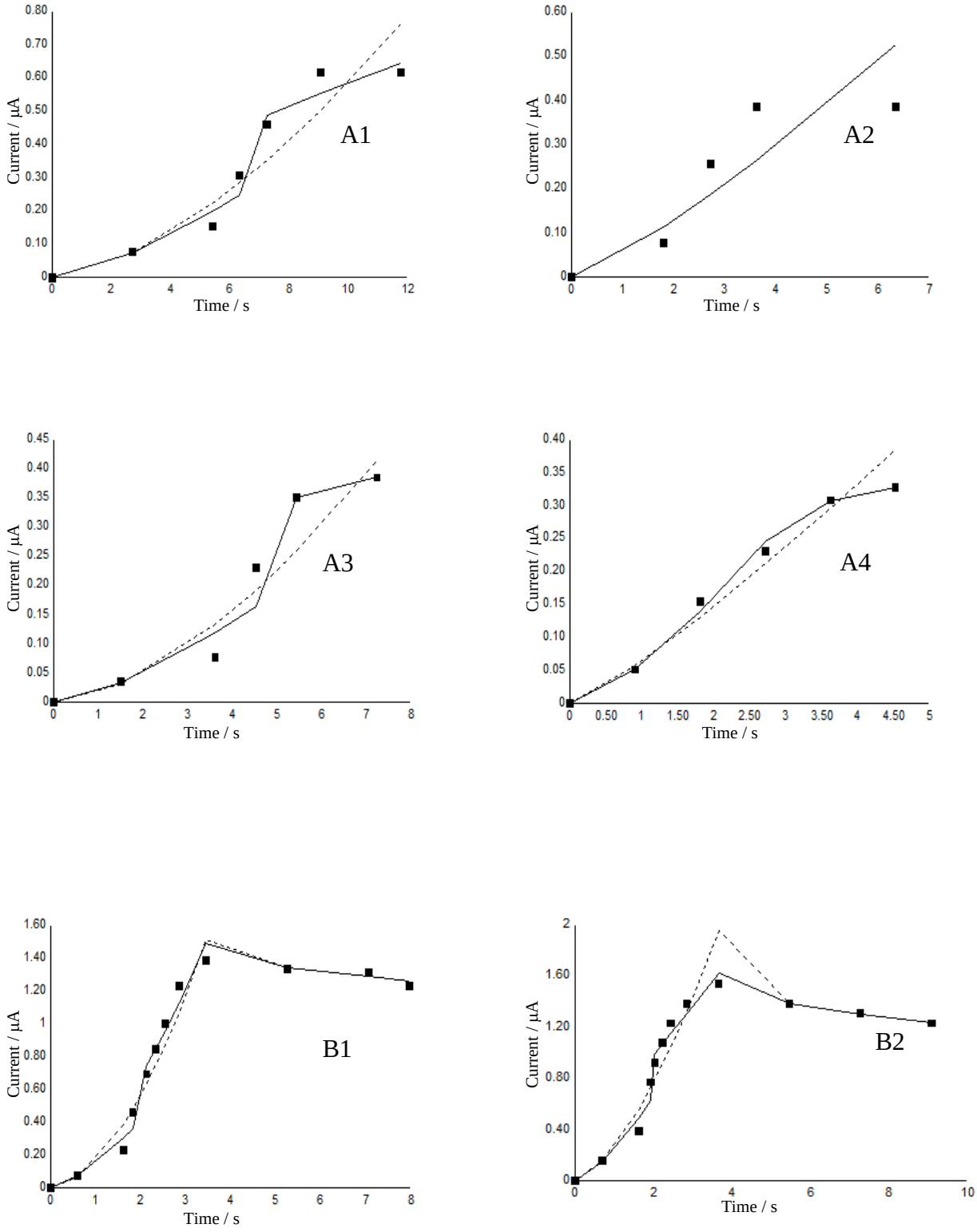


Figure 11: Binding and dissociation of different concentrations of glucose molecules (150 mM) in solution to 10 ml PBS (0.05 M, pH 6.8) with a +400 mV potential applied to a nanoparticle modified glucose sensor. (Sheng et al. 2009): (a) A1 – A4, 10 µl (b) B1 – B2, 33 µl

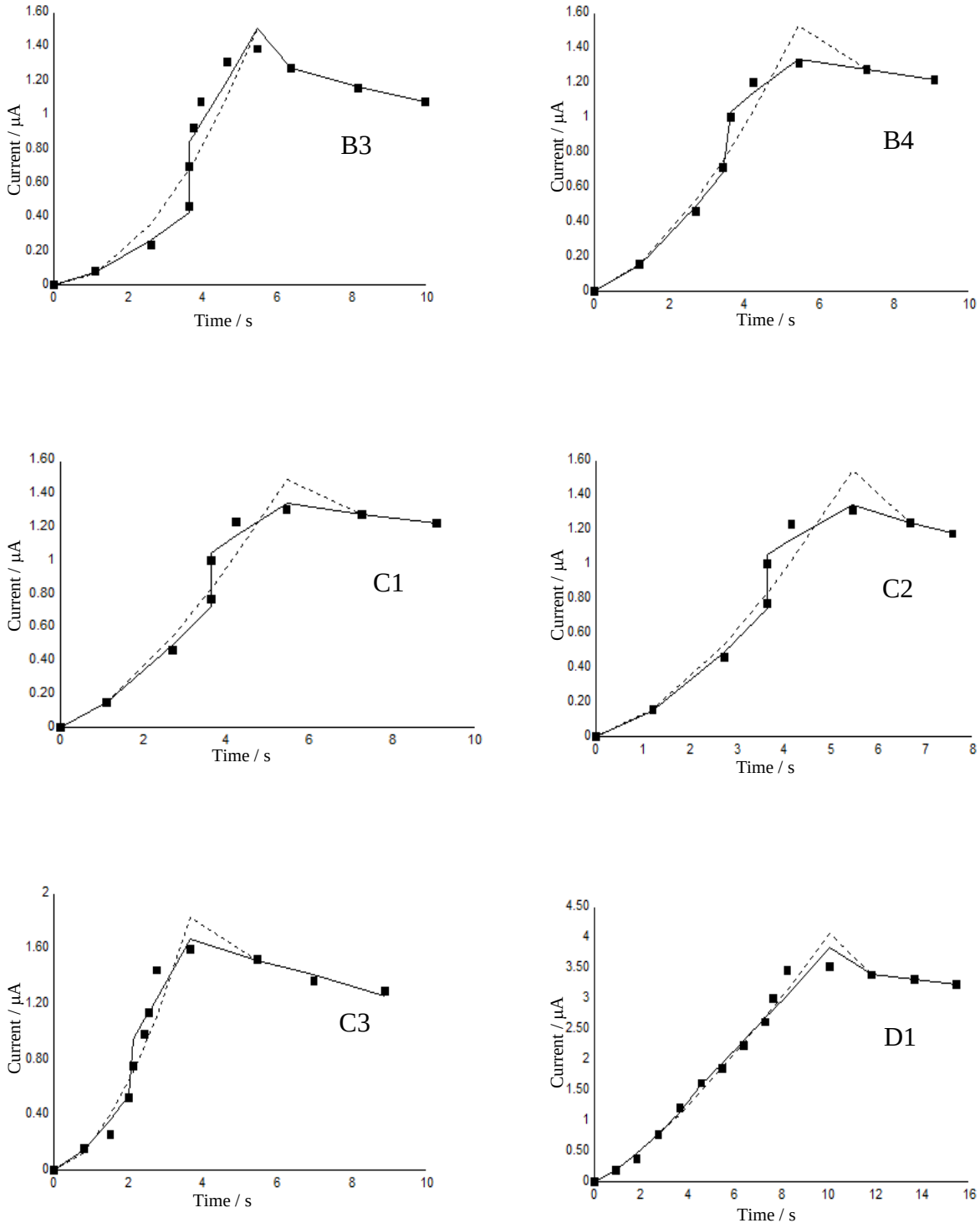


Figure 12: Binding and dissociation of different concentrations of glucose molecules (150 mM) in solution to 10 ml PBS (0.05 M, pH 6.8) with a +400 mV potential applied to a nanoparticle modified glucose sensor. (Sheng et al. 2009): (b) B3 – B4, 33 µl (c) C1 – C3, 100 µl (d) D1 >100 µl

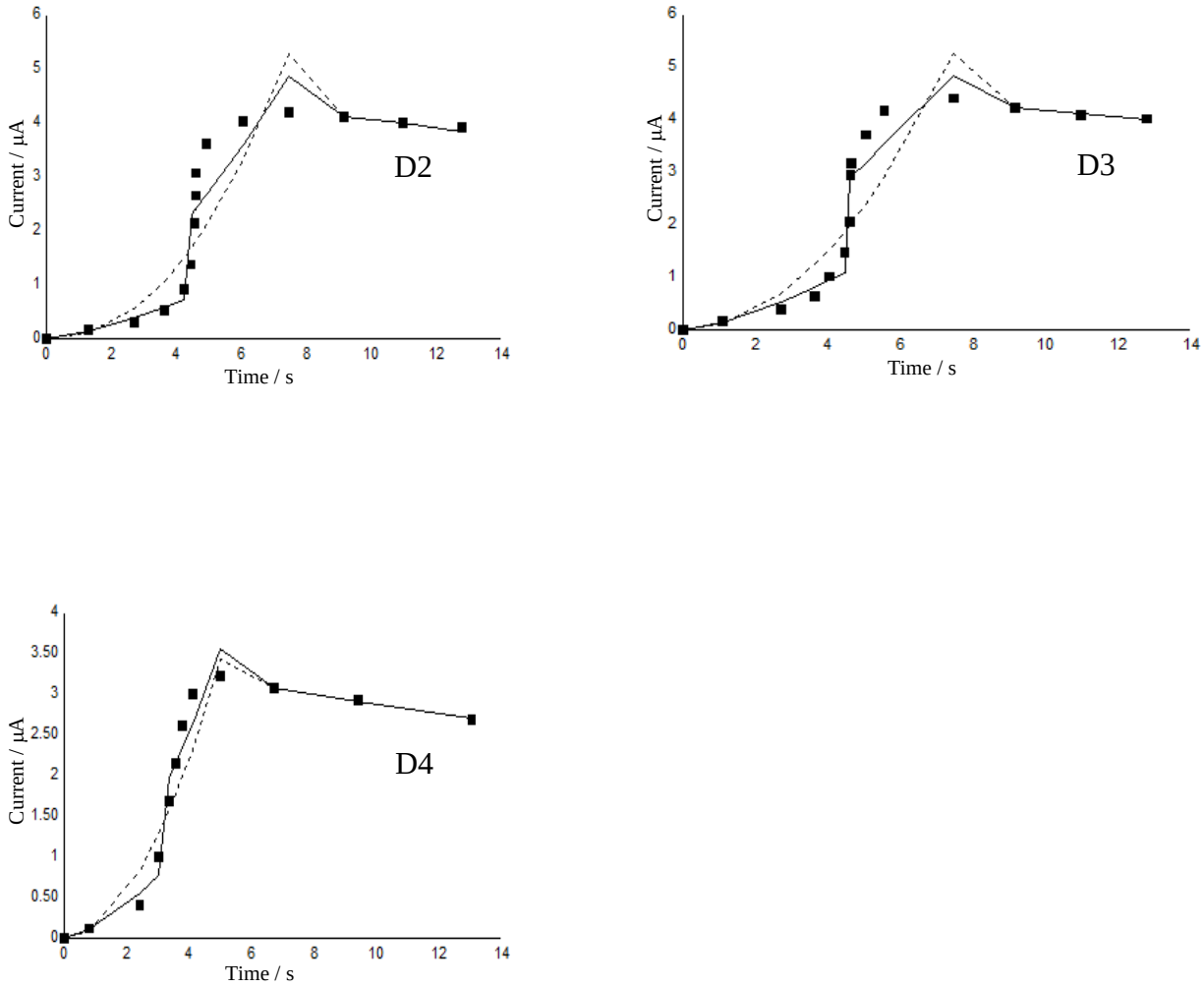


Figure 13: Binding and dissociation of different concentrations of glucose molecules (150 mM) in solution to 10 ml PBS (0.05 M, pH 6.8) with a +400 mV potential applied to a nanoparticle modified glucose sensor. (Sheng et al. 2009): (d) D2 – D4 >100 µl

| Analyte/Receptor | k | $k_1$ | $k_2$ | $k_d$ | $D_f$ | $D_{f1}$ | $D_{f2}$ | $D_{fd}$ |
|---|---|---|---|---|---|---|---|---|
| A1 | 0.015 ± 0.005 | 0.017 ± 0.007 | 0.156 ± 0.021 | na | na | 0.118 ± 1.057 | 1.848 ± 0.738 | na |
| A2 | 0.055 ± 0.035 | na | na | na | 0.546 ± 1.081 | na | na | na |
| A3 | 0.016 ± 0.008 | 0.018 ± 0.013 | 0.203 ± 0.000 | na | na | 0.077 ± 1.352 | 2.352 ± 0.000 | na |
| A4 | 0.065 ± 0.011 | 0.061 ± 0.008 | 0.214 ± 0.000 | na | 0.649 ± 0.250 | 0.218 ± 0.306 | 2.434 ± 0.000 | na |
| B1 | 0.162 ± 0.045 | 0.152 ± 0.068 | 0.248 ± 0.021 | 0.026 ± 0.010 | na | 0.126 ± 0.869 | 0.116 ± 0.433 | 0.895 ± 0.987 |
| B2 | 0.262 ± 0.062 | 0.243 ± 0.090 | 0.546 ± 0.039 | 0.106 ± 0.003 | na | 0.102 ± 0.830 | 1.324 ± 0.303 | 1.749 ± 0.066 |
| B3 | 0.054 ± 0.019 | 0.064 ± 0.011 | 0.131 ± 0.022 | 0.120 ± 0.003 | na | 0.069 ± 0.364 | 0.121 ± 0.906 | 1.725 ± 0.049 |
| B4 | 0.114 ± 0.020 | 0.115 ± 0.008 | 0.456 ± 0.030 | 0.014 ± 0.000 | na | 0.126 ± 0.178 | 1.735 ± 0.443 | 0.084 ± 0.000 |
| C1 | 0.129 ± 0.024 | 0.131 ± 0.013 | 0.467 ± 0.042 | 0.016 ± 0.000 | 0.123 ± 0.273 | 0.347 ± 0.212 | 1.755 ± 0.591 | 0.409 ± 0.000 |
| C2 | 0.115 ± 0.022 | 0.115 ± 0.008 | 0.488 ± 0.050 | 0.061 ± 0.000 | na | 0.119 ± 0.171 | 1.810 ± 0.664 | 0.890 ± 0.000 |
| C3 | 0.190 ± 0.054 | 0.194 ± 0.067 | 0.426 ± 0.062 | 0.038 ± 0.011 | na | 0.082 ± 0.772 | 0.893 ± 0.854 | 0.337 ± 0.664 |
| D1 | 0.211 ± 0.021 | 0.203 ± 0.025 | 0.289 ± 0.024 | 0.084 ± 0.002 | 0.438 ± 0.081 | 0.325 ± 0.180 | 0.759 ± 0.245 | 1.574 ± 0.057 |
| D2 | 0.093 ± 0.053 | 0.127 ± 0.044 | 0.558 ± 0.134 | 0.127 ± 0.006 | na | 0.142 ± 0.526 | 0.850 ± 1.023 | 1.642 ± 0.110 |
| D3 | 0.061 ± 0.039 | 0.105 ± 0.034 | 0.260 ± 0.093 | 0.038 ± 0.011 | na | 0.347 ± 0.629 | 0.086 ± 1.295 | 0.337 ± 0.664 |
| D4 | 0.149 ± 0.065 | 0.159 ± 0.078 | 0.317 ± 0.048 | 0.091 ± 0.006 | na | 0.151 ± 0.795 | 0.003 ± 0.910 | 1.334 ± 0.111 |

Table 6: Binding and dissociation rate coefficients and Fractal dimensions of different concentrations of glucose molecules (150 mM) in solution to 10 ml PBS (0.05 M, pH 6.8) with a +400 mV potential applied to a nanoparticle modified glucose sensor. (Sheng et al. 2009): (A) A1 – A4, 10 μl (B) B1 – B4, 33 μl (C) C1 – C3, 100 μl (D) D1 – D4 >100 μl

4.6 Biosensor based on polyaniline-Prussian Blue / multi-walled carbon nanotubes hybrid composites

Zou et al. (2007) constructed multi-walled carbon nanotubes (MWNTs) and combined these with Polyaniline-Praussian Blue (PANI-PB) to form a system of electrodes that amplified the sensitivity of $H_2O_2$ immensely. The authors then created a glucose biosensor by immobilizing glucose oxidase enzyme with Nafion and glutaraldehyde on the surface of the electrode. This immobilization process may have given rise to the microenvironment of the enzyme and hence affect the intrinsic properties to improve the affinity to glucose. They tested the sensor by successive addition of 1 mM glucose concentration at approximately 60 seconds gap with 0.1 M PBS +0.1 M KCl at 0.0 V.

The authors further tested the modified biosensor for interference tests by adding 1 mM of glucose followed by 0.2 mM ascorbic acid after 100 seconds and 0.2 mM L-cysteine. The results produced showed that the interference had either minimum effect or offered no change at all. These results lead to the conclusion of the biosensor showing rapid response, good reproducibility, high sensitivity and freedom from interference of other co-existing electro active species.

Figures 14 and 15 show the binding and dissociation of the glucose molecules to the biosensor made up of the modified composite electrodes. The glucose was added at equal time intervals of approximately 80 seconds and in successive concentrations of 1 mM glucose. A fractal analysis was carried out to model each of the peaks observed after addition of the stated glucose concentrations using the fractal equations for the binding and dissociation phases. A single fractal analysis was inadequate to describe the binding kinetics for each of the glucose concentrations; hence a dual-fractal analysis was applied. Since the concentrations of models A, B and F do not exhibit a “convex” nature close to the start of the

dissociation phase, their dissociation fractal dimension, $D_{fd}$, values are estimated and recorded in Table 7.

The values for (a) the binding rate coefficient, k, for a single fractal analysis, (b) the binding rate coefficients, $k_1$ and $k_2$ for a dual-fractal analysis, (c) the dissociation rate coefficient, kd, for a single-fractal analysis, (d) the fractal dimension, $D_f$, for binding for a single-fractal analysis, (e) the fractal dimensions, $D_{f1}$ and $D_{f2}$ for the binding for a dual-fractal analysis, and (f) the fractal dimension, $D_{fd}$ for the dissociation for a single-fractal analysis are presented in Table 7.

For all 3 models (A, B & F), the dissociation phase may be adequately described by a single-fractal analysis. This shows that there is no change in the dissociation kinetics mechanism for these 3 models in contrast to the dual-fractal analysis application to the binding kinetics. Also, as the dissociation rate coefficient, $k_d$, increases so does the dissociation fractal dimension, $D_{fd}$. The dissociation rate coefficient, $k_d$, exhibits a slightly different unit dependence on time (sec) for each of the values presented in Table 7 ($D_{fd}$ varies from 0.723 to 2.240). This is because of the factor, $(sec)^{(D_{fd}-3)}$.

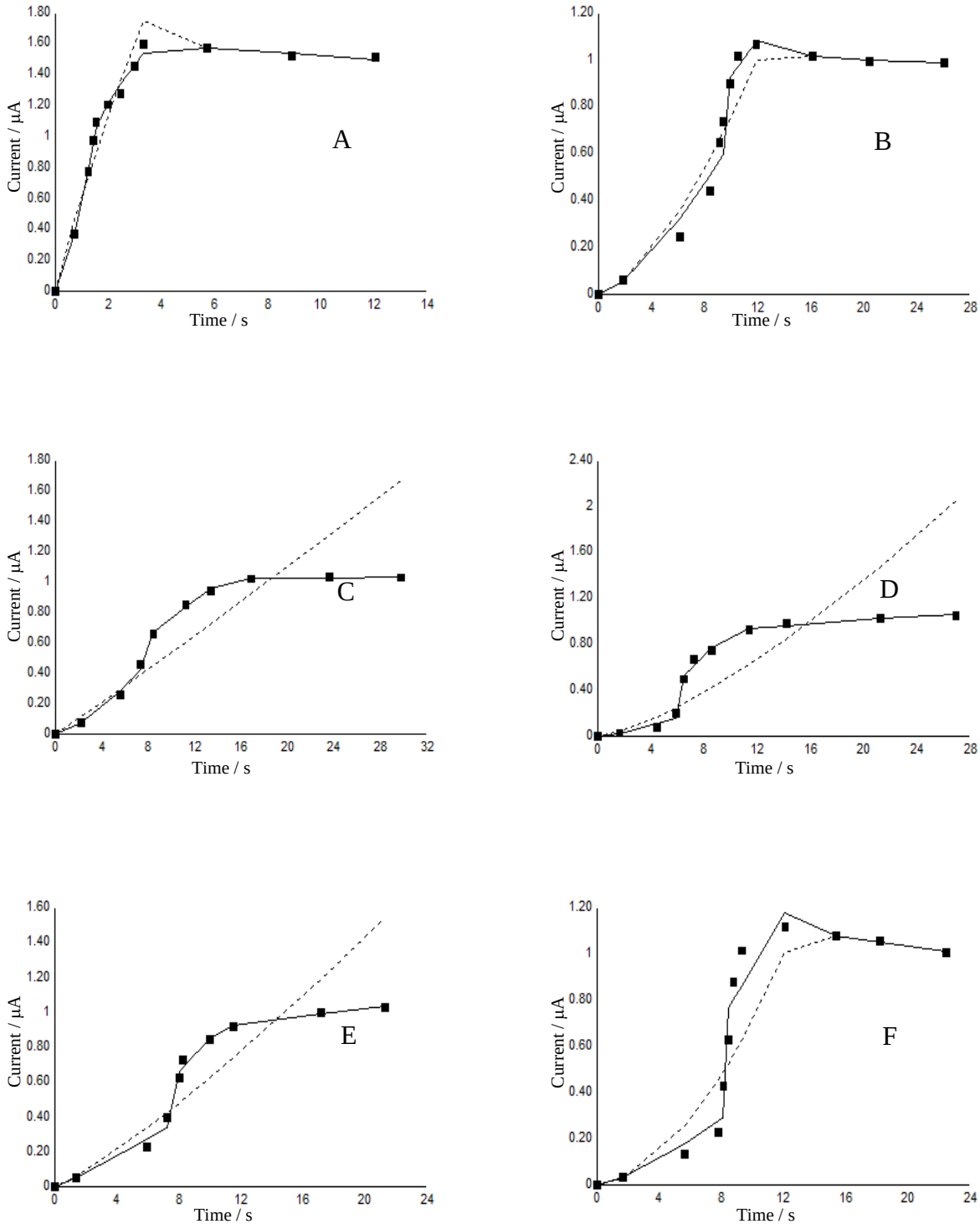


Figure 14: Binding and dissociation of different concentrations of glucose molecules (mM) in solution to 0.1M PBS (pH 6.5) and 0.1 M KCl at 0.0 V with a rotating rate of 3000 rpm. (Zou et al. 2007): Successive addition of 1 mM glucose Model A - F

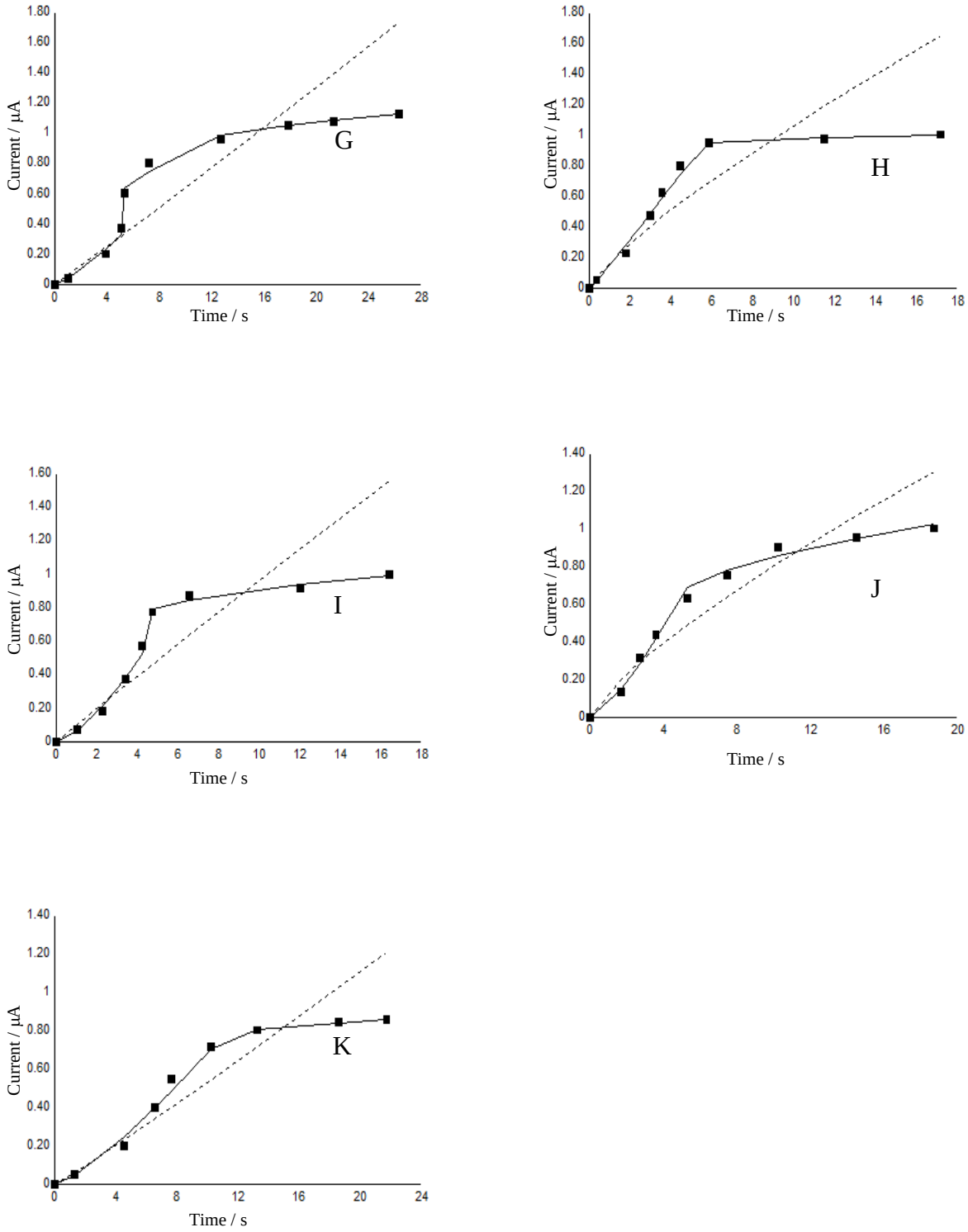


Figure 15: Binding and dissociation of different concentrations of glucose molecules (mM) in solution to 0.1M PBS (pH 6.5) and 0.1 M KCl at 0.0 V with a rotating rate of 3000 rpm. (Zou et al. 2007): Successive addition of 1 mM glucose Model G - K

| Analyte/Receptor | k | $k_1$ | $k_2$ | $k_3$ | $k_d$ | $D_f$ | $D_{f1}$ | $D_{f2}$ | $D_{f3}$ | $D_{fd}$ |
|---|---|---|---|---|---|---|---|---|---|---|
| A | 0.617 ± 0.097 | 0.590 ± 0.206 | 0.872 ± 0.032 | na | 0.008 ± 0.097 | 1.266 ± 0.217 | 0.304 ± 0.131 | 2.054 ± 0.117 | na | 0.723 ± 0.643 |
| B | 0.021 ± 0.006 | 0.035 ± 0.007 | 0.132 ± 0.008 | na | 0.030 ± 0.004 | na | 0.285 ± 0.339 | 1.298 ± 0.833 | na | 2.240 ± 0.288 |
| C | 0.048 ± 0.020 | 0.022 ± 0.003 | 0.123 ± 0.003 | 0.977 ± 0.005 | na | 0.910 ± 0.312 | 0.043 ± 0.294 | 1.418 ± 0.146 | 2.969 ± 0.024 | na |
| D | 0.022 ± 0.017 | 0.014 ± 0.007 | 0.039 ±0.005 | 0.651 ± 0.009 | na | 0.233 ± 0.475 | 0.270 ± 0.843 | 0.214 ± 1.140 | 2.704 ± 0.041 | na |
| E | 0.039 ± 0.015 | 0.034 ± 0.009 | 0.057 ± 0.005 | 0.584 ± 0.005 | na | 0.600 ± 0.292 | 0.678 ± 0.378 | 0.657 ± 0.993 | 2.627 ± 0.042 | na |
| F | 0.011 ± 0.007 | 0.017 ± 0.007 | 0.060 ± 0.013 | na | 0.011 ± 0.001 | na | 0.277 ± 0.567 | 0.613 ± 1.389 | na | 1.073 ± 0.135 |
| G | 0.060 ± 0.032 | 0.036 ± 0.007 | 0.273 ± 0.027 | 0.629 ± 0.003 | na | 0.948 ± 0.294 | 0.257 ± 0.304 | 1.985 ± 0.310 | 2.643 ± 0.031 | na |
| H | 0.167 ± 0.071 | 0.150 ± 0.023 | 0.876 ± 0.004 | na | na | 1.391 ± 0.227 | 0.861 ± 0.141 | 2.907 ± 0.013 | na | na |
| I | 0.102 ± 0.049 | 0.064 ± 0.009 | 0.597 ± 0.023 | na | na | 1.052 ± 0.335 | 0.072 ± 0.248 | 2.637 ± 0.077 | na | na |
| J | 0.136 ± 0.039 | 0.074 ± 0.010 | 0.437 ± 0.020 | na | na | 1.454 ± 0.226 | 0.316 ± 0.296 | 2.419 ± 0.129 | na | na |
| K | 0.046 ± 0.014 | 0.034 ± 0.005 | 0.571 ± 0.003 | na | na | 0.876 ± 0.225 | 0.377 ± 0.182 | 2.736 ± 0.032 | na | na |

Table 7: Binding and dissociation rate coefficients and Fractal dimensions of different concentrations of glucose molecules (mM) in solution to 0.1M PBS (pH 6.5) and 0.1 M KCl at 0.0 V with a rotating rate of 3000 rpm. (Zou et al. 2007): Successive addition of 1 mM glucose

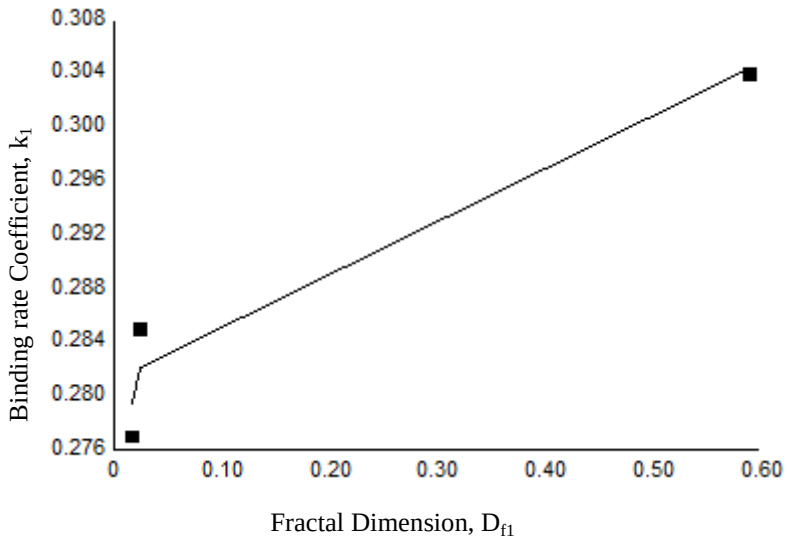


Figure 14a: Increase in the binding rate coefficient, $k_1$, with an increase in the fractal dimension for binding, $D_{f1}$.

The figure above (Figure 14a) shows that the binding rate coefficient, $k_1$, increases with an increase in the fractal dimension, $D_{f1}$. The binding rate coefficient, $k_1$, is given by:

$$k_1 = (0.308 \pm 0.004)\, D_{f1}^{(2.95 \pm 0.01)}$$

The binding rate coefficient, $k_1$, in this case exhibits a high sensitive to the degree of heterogeneity on the surface of the biosensor as can be noted by the 2.95 order of dependence on the fractal dimension, $D_{f1}$.

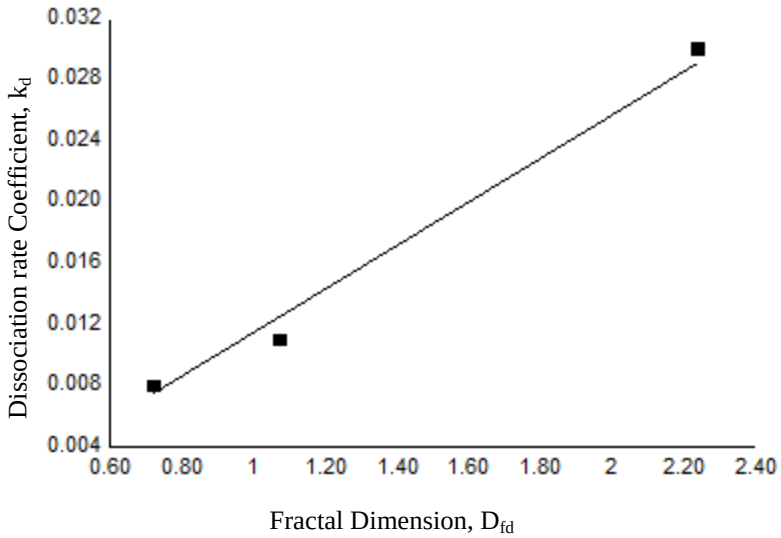


Figure 14b: Increase in the dissociation rate coefficient, $k_d$, with an increase in the fractal dimension for dissociation, $D_{fd}$.

The figure above (Figure 14b) shows that the dissociation rate coefficient, $k_d$, increases with an increase in the dissociation fractal dimension, $D_{fd}$. The dissociation rate coefficient, $k_d$, is given by:

$$k_d = (0.011 \pm 0.001)\, D_{fd}^{(0.61 \pm 0.28)}$$

The dissociation rate coefficient, $k_d$, in this case exhibits a moderate sensitive to the degree of heterogeneity on the surface of the biosensor as can be noted by the 0.61 order of dependence on the dissociation fractal dimension, $D_{fd}$. It is appropriate to analyze the values of binding and dissociation rate coefficients at this point. As stated by Germain (2001), if signal processing is to be promoted, then high values of binding rate coefficient, k, and lower values of dissociation rate coefficient, $k_d$, are desired. The high binding rate coefficients aid the binding process and the lower dissociation rate coefficients, provide the time required for the analyte-receptor complex on the surface of the biosensor to react with the co-receptor to develop a ternary complex and carry on the signal processing. The binding is occurring due

the increase in the heterogeneity of the surface of the biosensor by modulating the localized cell surface. However, in order for dissociation to take place, the degree of heterogeneity needs to be decreased and hence decreasing the dissociation coefficient. In our case the dissociation rate coefficient $k_d$ is decreasing with an increase in binding rate coefficient, $k_1$ as can be seen from Table 7. So an appropriate signaling can take place in this case.

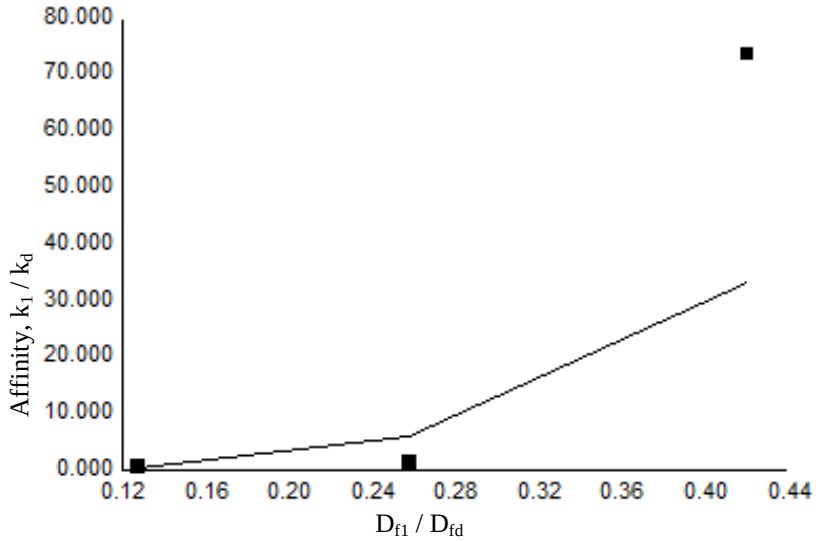


Figure 14c: Increase in the Affinity, $k_1/k_d$, with an increase in $D_{f1}/D_{fd}$.

The Affinity, K values are also calculated for this case. As can be seen in Figure 14c, there is an increase in affinity with an increase in fractal dimension ratio. Initially there is a slight increase of approximately 2-3 % which then sharply rises to over 100 times. Despite this there is a slight dependence for affinity, K on the unit dependence of time.

A regression analysis was performed on the second round of data recorded by Zou et al. (2007) on addition of (A) 1 mM glucose in solution to the sensor as shown in Figure 16. A single-fractal analysis is inadequate to describe the binding kinetics as can be seen from Figure 16 (represented by --- line). A dual-fractal analysis improves the fit and is adequate to describe the binding kinetics. The values for (a) the binding rate coefficient, k, for a single fractal analysis, (b) the binding rate coefficients, $k_1$, and $k_2$ for a dual-fractal analysis, (c) the fractal dimension, $D_f$, for binding for a single-fractal analysis, and (d) the fractal dimensions, $D_{f1}$ and $D_{f2}$ for the binding for a dual-fractal analysis are presented in Table 8. Since there is no dissociation phase occurring here, no affinity values are presented.

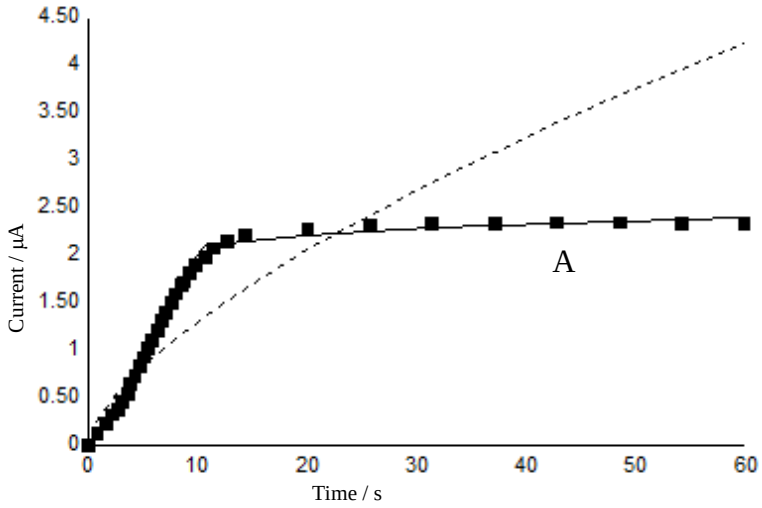


Figure 16: Binding of 1.0 mM of glucose in solution to 0.1M PBS (pH 6.5) and 0.1 M KCl at 0.0 V with a rotating rate of 3000 rpm followed by addition of 0.2 mM ascorbic acid. (Zou et al. 2007)

| Analyte/Receptor | k | $k_1$ | $k_2$ | $D_f$ | $D_{f1}$ | $D_{f2}$ |
|---|---|---|---|---|---|---|
| A | 0.283 ± 0.121 | 0.129 ± 0.009 | 1.743 ± 0.048 | 1.678 ± 0.122 | 0.607 ± 0.048 | 2.843 ± 0.026 |

Table 8: Binding rate coefficient and Fractal dimension of 1.0 mM of glucose in solution to 0.1M PBS (pH 6.5) and 0.1 M KCl at 0.0 V with a rotating rate of 3000 rpm followed by addition of 0.2 mM ascorbic acid. (Zou et al. 2007)

# CHAPTER 5

## CONCLUSIONS

A fractal analysis for the binding of glucose molecule in solution to glucose oxidase enzyme in most cases immobilized on the biosensor provides the rate of binding and dissociation coefficient, k and $k_d$, and the degree of heterogeneity by the use of the fractal dimension, $D_f$ for both the phases. The fractal analysis provides a kinetic analysis of the diffusion-limited reactions occurring on structured or heterogeneous surfaces.

The data presented by all the authors is shown in the result section of this thesis and is re-analyzed to provide binding and dissociation rate coefficients and link them with the degree of heterogeneity that exists on the surface of the biosensor. Obtaining these values enable us to determine the type of kinetics occurring at the surface of the biosensor, hence allowing the generation of an overall picture. The affinity value, K, obtained can be used to enhance beneficial reactions of glucose receptors. All three fractal analysis; single, dual and triple are used to adequately model the binding kinetics, while a single-fractal was adequate for the dissociation kinetics in the cases applicable. The triple-fractal analysis is only used when the dual-fractal analysis isn't adequate enough to provide an appropriate fit and the dual-fractal analysis is used only when the single-fractal analysis does not provide an adequate fit (least squares sum less than 0.97). The modeling was done on Quattro Pro X5 (2010).

In most of the cases there was a slight dependence of the binding rate coefficient on the fractal dimension value. Some of the cases (Serra et al. 2007 and Sheng et al. 2009) did

not exhibit any direct relation with the binding rate coefficient and fractal dimensions, these cases could have portrayed such results due to numerous factors including inadequate jiggered fits, human error and inaccurate data recording for analysis. In relation with the prefactor analysis for fractal aggregates (Sorenson et al. 1997), quantitative expressions are developed for the binding and dissociation coefficients as a function of the binding and dissociation fractal dimensions of the glucose molecule with the glucose oxidase enzyme immobilized on the surface of the biosensor.

The fractal dimensions for both these phases are dependent on various factors including the concentration of analyte in solution (more applicable to this case) and the receptor on the surface of the biosensor. It is calculated from the equations 3a-3e stated in the theory section of the thesis and is considered as a derived variable. It is safe to assume that there is a direct linkage between the rate of binding and dissociation coefficient and the degree of heterogeneity on the surface of the biosensor. The link between concentration can only be observed in four out of six of the above cases, where applicable a relation between the fractal dimension and the binding and / or dissociation coefficient have been graphically presented to exhibit the direct relationship.

Although the analysis provided is that for the analyte-receptor reaction-taking place on the surface of the biosensor, it does give an idea of how the reaction occurs on the actual cellular surface. A broader range of analysis is required to determine if the binding and dissociation rate coefficients are sensitive to the degree of heterogeneity that exists on the surface of the biosensor and can be observed by the higher orders of dependence. Martin et al. (1993) stated that fractals on surface lead to turbulence that accelerated mixing, hence decreasing the diffusion limitations that in turn leads to an increase in the binding and dissociation rate coefficients. For this to take place, the length of the turbulent boundary layer may have to extend a few single layers above the surface of the sensor to influence the bulk

diffusion to and from the surface. Although this only occurs if the more common laminar flow in most biosensors is absent.

The surface of a fractal is consisted of ridges and grooves; this nature of the surface may lead to diffusion by eddy movements. This eddy diffusion aids the mixing on the surface, thereby extending the length of the boundary layer allowing bulk diffusion to take place to and from the surface of the biosensor. To further influence the binding and dissociation coefficients cells may be introduced to toggle the degree of heterogeneity in the desired direction.

To conclude, further understanding the analyte-receptor relationship in relationship to the heterogeneity on the surface of the biosensor can lead to development of more efficient and quicker ways of monitoring glucose levels and can in turn aid in early curing of one of the most common disease Diabetes mellitus (DM).

# BIBLIOGRAPHY

1. Sadana, A. and Sadana, N., "Handbook of Biosensors and Biosensor Kinetics," 1st ed. Oxford (UK): Elsevier; 2011
2. Galan-Vidal, C.A., Munoz, J., Dominguez, C. and Alegret, S., (1997), "Glucose biosensor based on a reagentless graphite-epoxy screen-printable biocomposite," Sensors and Actuators 45: 55-62
3. Zou, Y., Sun, Li-X. and Xu, F., (2007), "Biosensor based on polyaniline-Prussian Blue/multi-walled carbon nanotubes hybrid composites," Biosensors and Bioelectronics 22: 2669-2674
4. Serra, P.A., Rocchitta, G., Bazzu, G., Manca, A., Puggioni, G.M., Lowry, J.P. and O'Neill, R.D., (2007), "Design and construction of a low cost single-supply embedded telemetry system for amperometric biosensor applications," Sensors and Actuators 122: 118-126
5. Zeng, G-M., Tang, L., Shen, G-L., Huang, G-H. and Niu, C-G., (2004), "Determination of trace Chromium(VI) by an inhibition-based enzyme biosensor incorporating and electropolymerized aniline membrane and ferrocene as electron transfer mediator," Intern. J. Environ. Anal. Chem. Vol. 84, No. 10: 761-774
6. Sheng, Q., Luo, K., Li, L. and Zheng, J., (2009), "Direct electrochemistry of glucose oxidase immobilized on $NdPO_4$ nanoparticles/chitosan composite film on glassy carbon electrodes and its biosensing application," Bioelectrochemistry 74: 246-253
7. Norouzi, P., Faridbod, F., Larijani, B., and Ganjali, M.R., (2010), "Glucose Biosensor based on MWCNTs-Gold nanoparticles in a Nafion Film on the glassy carbon electrode using Flow injection FFT continuous cyclic voltammetry," Int. J. Electrochem. Sci.,5: 1213-1224
8. Sienko, T., Adamatzky, A., Rambidi, N.G. and Conrad, M., "Molecular Computing," Cambridge, Massachusetts (USA): MIT Press; 2003.

9. Havlin, S., (1989), “Molecular diffusion and reactions,” in The Fractal Approach to Heterogeneous Chemistry: Surfaces, Colloids, Polymers, Avnir, D. (Ed.), J Wiley & Sons: New York, 251-269
10. Pfeifer, P. and Obert, M., (1989), “In The Fractal Approach to Heterogeneous Chemistry: Surfaces, Colloids, Polymers,” Avnir, D. (Ed.), J Wiley & Sons: New York, 251-269
11. Kopelman, R., (1988), “Fractal Reaction kinetics,” Science 241: 1620-1624
12. Markel, V.A., Muratov, L.S., Stockman, M.I. and George, T.F., (1991), “Theory and numerical simulation of optical properties of fractal clusters,” Physics Reviews B 43(10): 8183
13. Suleiman, A. and Guilbault, G., (1991), “Piezoelectric (PZ) immunosensors and their applications,” Analytical Letters 24(8)
14. Byfield, M.P., Abuknesha, R.A., (1994), “Biocehmical aspects of biosensors,” Biosens. & Bioelectron 9(4-5): 373-400
15. Yoo, E. and Lee, S., (2010), “Glucose Biosensors: An overview of use in clinical practice,” Sensors 10: 4558-4576
16. Chaplin, M. and Bucke, C., “Enzyme Technology,” Cambridge (UK): Cambridge University Press; 1990
17. Li, H., Wang, F. and Zhao, H., (1995), “Fractal reactions on enzyme surfaces,” Huaxue Wuli Xuebao 8(2): 162-8
18. Sadana, A. and Chen, Z., (1996), “Influence of non-specific binding on antigen-antibody binding kinetics for Biosensor Applications,” Biosens. & Bioelectron. 11(8): 769-782
19. Sadana, A., (2001), “A kinetic study of analyte-receptor binding and dissociation,” Anal. Biochem. 291(1): 34

20. Sadana, A., Ramakrishnan, A. and Vontel, S., (2000), “An evaluation of hybridization kinetics in Biosensors using a Single Fractal Analysis,” Biotechnol. & Appl. Chem. 31(2): 161
21. Hutchison, K.A., Stancato, L.F., Owens-Grillo, J.K., Johnson, J.L., Krishna, P., Toft, D.O. and Pratt, W.B., (1995), “The 23 kDa acidic protein in reticulocyte lysate is the weakly bound component of the hsp foldosome that is required for assembly of the glucocorticoid receptor into a functional heterocomplex with hsp90,” Biol. Chem. 270: 18841-18847
22. Knoblauch, R. and Garabedian, M.J., (1999), “Role for Hsp90-associated cochaperone p23 in Estrogen receptor signal transduction,” Mol. Cell. Biol. 19: 3748-3759
23. Biacore AB, 2002. BIAevaluation, 3.2 software, Uppsala, Sweden
24. Lowry, J.P., Miele, M., O’Neill, R.D., Boutelle, M.G. and Fillenz, M., (1998), “An amperometric glucose-oxidase/poly(o-phenylenediamine) biosensor for monitoring brain extracellular glucose,” J. Neurosci. Methods 79(1): 65-74
25. Weisstein, Eric W. "Fractal." From MathWorld--A Wolfram Web Resource. http://mathworld.wolfram.com/Fractal.html
26. Karube, I., Turner, A.P.F. and Wilson, G.S., “Biosensors: Fundamentals and Applications,” Moscow: Mir Publishers; 1992
27. Mandelbrot, B.B., (1967), “How long is the coastline of Britain? Statistical self-similarity and fractional dimension,” Science 156: 636-638
28. Mandelbrot, B.B., “The fractal geometry of nature,” New york (USA): W. H. Freeman & Co.; 1983
29. Clarke, A.C., (1995) “The colors of infinity,” documentary

30. Chaudhari, A., Yan, C.C. and Lee, S.L., (2002) “Multifractal analysis of diffusion-limited reactions over surfaces of diffusion-limited aggregates,” Chemical Physics Letter 207: 220-226
31. Coppens, M.O. and Froment, G.F., (1995), “Diffusion and reaction in a fractal catalyst pore. Geometric aspects,” Chemical Engineering Science 50(6): 1013-1026
32. Havlin, S. and Ben-Avraham, D., (1987), “Diffusion in disordered media,” Advance in Physics 36: 695-798
33. Vijayendran., R.A. and Leckband, D.E., (2001), “A quantative assessment of heterogeneity for surface-immobilized proteins,” Analytical Chemistry 73: 471-480
34. Koopal, L.K. and Vos, C.H.W., (1993), “Adsorption on heterogeneous surfaces. Calculation of the adsorption energy distribution function or the affinity apectrum,” Langmuir 9: 2593-2605
35. Cooper, M.A, (2002), “Optical biosensors in drug discovery,” National Reviews in Drug Discovery 1: 515-528
36. Giona, M., (1992), “First-order reaction-diffusion in complex fractal media,” Chemical Engineering Science 47: 1503-1515
37. Germain, R.N., (2001), “The art of the probable: System control in the adaptive immune system,” Science 293(5528): 240-245
38. Sorenson, C.M. and Roberts, G.C. , (1997), “The prefactor of fractal aggregates,” J. Colloid & Interface Sci. 186: 447-453

# VITA

Lokesh Taneja was born in Nairobi, Kenya, on October 18, 1985. After completing High school in Nairobi, Kenya, he went on to graduate from the University of Nottingham (UK) with a Bachelor of Engineering (Honors) in mechanical engineering. He then enrolled in Illinois Institute of Technology (Chicago) to pursue masters in Chemical Engineering and after one semester, transferred down to Ole Miss to complete his graduation in Masters of Science in Chemical Engineering in May 2012. He has secured a job after graduation with an Oil & Gas company as a Product Development and Design engineer in the subsea compartment. He is a member of the IMechE (Institution of Mechanical Engineers) and AIChE (American Institute of Chemical Engineers).